**Abstract**

Entangled photons are useful for both error correcting of quantum signals travelling over long transmission distances and in quantum computing. One method of creating such photons is a protocol relying on the driving of transitions in a three-level quantum system. The possibility of a fourth level necessitates the optimisation of the length of the pulse, which is used to drive the frequencies, and this requires the calculation of the coefficients of the system. An analytical description of this is attempted at both in a bare state basis and a dressed state basis but the results are both found not to correspond with the numerical solutions. In the case of the dressed state basis, the differential equations can be rewritten as an integral, but this integral cannot be solved analytically without the use of approximations that do not hold for most pulses. Further investigations has not been able to provide a satisfactory description of the system.

**Acknowledgements**

I would like to thank my supervisor Anders Sørensen for help and guidance both in person and over an unspeakable number of emails, and Konstantin Tiurev for the time he took to help me with explanations and debugging. Furthermore, I would like to thank my family and friends for emotional support and proof reading.

# Contents

# 1 Introduction

Quantum information builds on the idea of using quantum system as the basis for information theory and thus utilise the many strange properties of quantum mechanics in communication and information processing. It is a rapidly developing field, that move towards the actual realisation of quantum computers, which will have computation speeds that challenges the foundation of today's secure coding. But before reaching such heights a thorough theoretical groundwork needs to be lain, including the problem of dealing with losses during transmissions over long distances. This thesis concerns itself with this problem by investigating a protocol used to generate entangled multi-photon states that can in turn be used both in quantum computation and for a certain kind of quantum repeater, that are used to correct errors along the transmission of a quantum signal.

In the next section a short overview of quantum information theory in general is presented together with examples of the uses for entangled photon clusters. This will serve as a motivation for the production of entangled photons, which is the purpose of the protocol which will be described in section 2. This protocol rely on driving frequencies in a three-level quantum system, however, there is a non-zero probability of also driving transitions to a fourth level, and this is further investigated. More specifically, an attempt is made to calculate the coefficients describing transitions to this fourth level, which is far-detuned from the laser light used in the protocol. To do this perturbation theory is used on descriptions of the system in different bases. This however, turns out to be futile, as the approximations needed for an analytical answer, are not good enough. Some further investigations is made into how these descriptions fail, and into the possibility of finding other kinds of approximate descriptions of the system. The error caused by spontaneous decay of this far-detuned two-level system is also calculated.

Throughout this thesis natural units are used, meaning that $c = \hbar = \epsilon_0 = 1$.

# 2 Quantum Information

Information theory is a probabilistic theory. The information that is to be gained from a system, $A$, is defined as the information entropy, which is in turn given by the probabilities, $P$, of the system having different measurement outcomes, $a_i$. The information entropy corresponds to thermodynamical entropy when multiplied with Boltzmanns constant, and the expression is given in equation 1.

$$H = -\sum_i P(a_i) \log P(a_i) \tag{1}$$

When the base of the logarithm is 2, the information is counted in units of "bits". This expression is at maximum, when the probabilities $P(a_i)$ are all equal, which corresponds to knowing nothing about what outcome a measurement of $A$ is likely to give. In information theory binary systems, i.e. systems with only two possible measurement outcomes 0 and 1, are used. Such a system reaches its maximum of information of one bit, when the probabilities are $P(1) = P(0) = \frac{1}{2}$, and because of this, the binary system itself (when prepared with these probabilities) is often referred to as a bit. [2]

Quantum mechanics is a probabilistic theory as well, and considering this it is not surprising that quantum information, which is information theory of quantum systems rather than classical systems, has been developed. In quantum information theory, the classical bit is replaced by a so called qubit, which is a quantum system which has two orthogonal states $|0\rangle$ and $|1\rangle$. As opposed to the classical bit, the qubit has the possibility of being in a superposition of these states, $c_0|0\rangle + c_1|1\rangle$, where $c_0$ and $c_1$ are (complex) coefficients that gives the probability of the qubit being found in respectively states $|0\rangle$ and $|1\rangle$ upon measurement as $P_i = |c_i|^2$. [2]

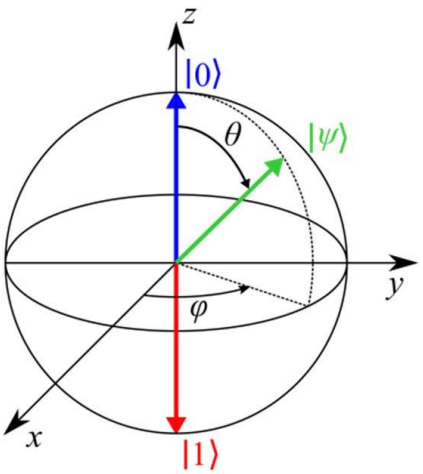


Figure 1: An illustration of the Bloch sphere. A quantum state $|\Psi\rangle$ is given as a Bloch vector (green), which can be rotated by angles $\theta$ and $\phi$ by unitary operations. Figure taken from [1].

In quantum mechanics operators are given by matrices, and
the state of a qubit can be changed by applying such a unitary operator. Unitarity means that an operator, $\hat{U}$, the product $\hat{U}\,\hat{U}^\dagger = \hat{I}$, where $\hat{U}^\dagger$ is the adjoint matrix and $\hat{I}$ is the identity matrix. [3] A convenient way of describing the state of a quantum system is as a so called Bloch vector, where the state of the system is pictured as a three-dimensional vector, with components given by equation 2, where $\rho_{nm}$ are components of the density matrix, $|\Psi\rangle\langle\Psi|$, which gives the squared coefficients and the coherences of the state of the system. [4]

$$\begin{aligned} u &= \rho_{12} + \rho_{21} \\ v &= -i(\rho_{12} - \rho_{21}) \qquad \text{, where} \quad \begin{pmatrix} \rho_{11} & \rho_{12} \\ \rho_{21} & \rho_{22} \end{pmatrix} = |\Psi\rangle\langle\Psi| = \begin{pmatrix} |c_0|^2 & c_0 c_1^* \\ c_1 c_0^* & |c_1|^2 \end{pmatrix} \\ w &= \rho_{11} - \rho_{22} \end{aligned} \tag{2}$$

In this picture, unitary operators describe rotations on the surface of the Bloch sphere. An example is a pulse of light that changes the state from $|0\rangle$ to $|1\rangle$ corresponding to a rotation of $\pi$. Such a pulse is therefore known as a $\pi$-pulse, and corresponds to a pulse where the integral of the intensity over time is equal to $\pi$. A $\frac{\pi}{2}$-pulse has an integral equal to $\frac{\pi}{2}$, and rotates the Bloch vector by $\frac{\pi}{2}$, thus making a pure state $|0\rangle$ into a superposition $\frac{1}{\sqrt{2}}(|0\rangle + |1\rangle)$. [4] An illustration of the Bloch sphere is given in figure 1.

A quantum information problem can involve more than one quantum system, and in this case the state is written as in equation 3, where $\otimes$ denotes the tensor product.

$$|\Psi\rangle = |\lambda\rangle \otimes |\phi\rangle \tag{3}$$

For such a mixed state, the operation $\hat{A} \otimes \hat{B}$, where $\hat{A}$ and $\hat{B}$ are unitary operators, acting on $|\Psi\rangle$, results in the state given in equation 4.

$$(\hat{A} \otimes \hat{B})|\Psi\rangle = (\hat{A}|\lambda\rangle) \otimes (\hat{B}|\phi\rangle) \tag{4}$$

In the state described in equation 3, $|\lambda\rangle$ and $|\phi\rangle$ can be treated as two individual quantum systems, however, this is not the case in equation 5.

$$|\Psi\rangle = \sum_n a_n |\lambda_n\rangle \otimes |\phi_n\rangle \tag{5}$$

Equation 5 is also a possible state as it is a superposition of possible states. [3] A state of this kind cannot be written as a (tensor) product of states, and is for this reason defined as an entangled state. For the state in equation 3, the expectation values of operators $\hat{A}$ and $\hat{B}$ associated with each of the systems $|\lambda\rangle$ and $|\phi\rangle$, will satisfy equation 6, as the operation works in accordance with equation 4.

$$\langle\Psi|(\hat{A} \otimes \hat{B})|\Psi\rangle = \langle\Psi|\hat{A}|\Psi\rangle\langle\Psi|\hat{B}|\Psi\rangle \tag{6}$$

But this is not the case for entangled states, as the (tensor) product of the operators do not factorise in this way. This means that some properties of two entangled systems are correlated and cannot be determined individually. Correlations of properties also exist in classical mechanics, however entangled systems exhibit forms of correlations, that cannot be explained by classic mechanics, such as the instantaneous change of state of one system caused by the measurement upon the other. These effects can be exploited in quantum information, if two entangled qubits, called an ebit, are used. [2]

## 2.1 Quantum communication

Quantum communication describes the process of sending a message from a sender, in general called Alice, to a receiver, in general called Bob, via a quantum system. A quantum communication begins with Alice choosing a message, represented by a certain state of a qubit. This qubit is sent to Bob, who then needs to determine what state the system is in in order to receive the message. If the possible states of the system are mutually orthogonal, this can be done by the measurement of an observable, but this is generally not the case due to the possibility of the system being in a state of superposition. Thus it is not always possible to determine which state the system was in from the measurement outcome, and furthermore, it matters in what basis the measurements are made, and thus Bob has a choice of several different bases when receiving the qubit. [2]

Interference with the quantum system during the transportation from Alice to Bob destroys the information carried, as it acts as a measurement of the state and thus collapses the superposition (with exception of rare cases of the state being an eigenstate of the measured property). This however, also acts as a protection from a possible eavesdropper, generally referred to as Eve. The no-cloning theorem [2] renders it impossible for Eve to exactly clone the quantum state, thus preparing a second qubit, that can be sent to Bob, while she can conduct measurements upon the original qubit. It is therefore neither possible for Eve to measure or to clone the qubit without changing it's state and thus allowing detection of her activities. This feature is exploited in quantum key distribution, where a key, i.e. some bit string, needs to be known by both Alice and Bob without the possibility of detection by Eve. It works by Alice randomly preparing a sequence of quantum systems in one of two eigenstates in one of two possible bases. She takes note of what the states are before sending them to Bob, who then measures the states of all the systems choosing random bases. Alice and Bob compares the bases they used over a classical channel (where it is assumes that Eve can eavesdrop without detection), but do not tell the measurement outcome. All bits where different bases was used are discarded. To check if any eavesdropper has been present, who could in that case know that part of the sequence where she too used the same basis, Alice and Bob compares a part of the sequence. If they do not correspond exactly this is in principle a proof of the presence of the eavesdropper. In reality, however, it is a question of judging how much discrepancy can be tolerated, as noise is bound to result in some degree of error. The part of the sequence which is compared is later discarded, but the remaining part is vouched safe to use as a secret key, if the sequence, that was compared, passed the test for eavesdroppers. [2]

The maximum amount of information of a qubit is one bit, as is the case with a classical binary system. However the possibility of Alice and Bob sharing an ebit, that is to say each having one of a pair of entangled qubits, makes it possible for Alice to communicate two bits of information, by just sending her one qubit to Bob. This is known as quantum dense coding, and exploits the fact that Alice, by performing operations on her own qubit can change the state of the entangled system, and thus the outcome of Bob's measurement upon receiving her qubit. As Alice can change the state of not only her own qubit but of both qubits, two classical bits of information is contained in the measured state. [2]

Ebits also enable communication of one bit of information without the transmision of any physical qubit. This is known as teleportation. No physical object is transported, but quantum information is passed from one system to another, by changes in the state vector of the combined, entangled system. For this process an ebit is shared between Bob and Alice, who wants to communicate the state of an additional qubit. Alice can prepare Bob's qubit in a state, which depends on the state of her additional, non-entangled qubit by conduction measurements upon her both of her qubits. By then telling Bob in what basis he has to measure his own qubit, which will require the classical communication of two bits, it is possible to create a copy of Alice's non-entangled qubit, and thus communicating the one qubit of information it contains. As Alice performs measurements on her qubits, the information that was contained in the state of the non-entangled qubit is erased. Thus the state is communicated and not copied, in accordance with the no-cloning theorem. [2]

Both quantum dense coding and teleportation has the advantages of being secure from eavesdroppers, as the shared ebit between Alice and Bod is required for communication to take place.

## 2.2 Quantum Repeaters

If quantum information is to be utilised in reality, qubits needs to be transmitted over long distances and thus facing the problem of transmission loss. For classical communication channels it is possible to amplify the signal, however this is not the case for quantum communication due to the no-cloning theorem. In order to solve this problem the idea of quantum repeaters has been proposed. Quantum repeaters are placed along the transmission channel, and thus divides the distance that the qubit needs to travel into smaller parts between which errors due to loss are corrected. Traditionally, quantum repeaters rely on pre-established entangled states shared between neighbouring quantum repeaters and requires two-way communication between the repeaters. Another type, called one-way quantum repeaters, does not, however, utilise pre-esteblished entangled links between the repeaters. For this type of quantum repeater the quantum information is encoded onto a multitude of physical qubits, e.g. photons. Even though some are lost, the remaining qubits can be used to restore the entire amount at each repeater. [5][6]

One specific type of quantum repeater use photonic tree-cluster states onto which one qubit of information is encoded. Cluster states are complicated multi-qubit entangled states which has some specific properties determining how a measurement of one qubit, will leave the remaining qubits in a new cluster state. [7]. A certain type of cluster

state, tree clusters, exploit these properties in order to create branches of entangled links. The state of the qubit that is to be transmitted is encoded in the entangled state of such a tree cluster state, by making measurements that results in teleportation of information into the entangled state. The cluster is then transmitted to the next repeater station. Here the state of the original qubit can retrieved, and the process of encoding the state into a new photon cluster is repeated, and the photons transmitted to the next repeater station, and so forth. This can be done even though some photons are lost during the transmission and also enables error correction at each repeater station. [5] In fact, when using these states, the quantum repeaters can work with as little as two memory qubits and one quantum state, which can emit photons, per repeater. Furthermore error correction can be done by only one measurement. [5] Thus the creation of photonic cluster states is highly relevant for the realisation of quantum communication.

### 2.3 Quantum Computation

Quantum systems can be used for containing information and as different operators changes the states of the qubits they can be used as different logical gates. In this way it is possible to process quantum information , and thus the foundations of quantum computation are laid. A string of qubits can be used as input data, which is acted upon by a series of quantum gates, and is at last measured in some suitable basis, thereby given the output data. This differs from a classical computing process by allowing the state of the qubit to be a superposition of the computational basis states, $|0\rangle$ and $|1\rangle$, and by it not being possible to conduct a measurement on the qubit during the computation process, as this would collapse the state of the qubit. Quantum computating has several advantages over classical computation, which mainly arises from the possibility of each qubit being not only in one state, but in a superposition of many states. By performing an operation on such a qubit, the transformed values of all basis states are calculated simultaneously, as all are present in the transformed superposition state. This greatly increases the speed of quantum computations as opposed to classical computation. [2]

One approach to quantum computing is to use photons as the qubits, but as photon-photon interaction is quite weak it is a challenge to perform operations with only two photons. There is, however, the possibility of using entangled states of multiple photons, by which optical quantum computing becomes feasible. [8] Optical quantum computing can be useful, as it greatly reduces stochastic noise, because of technical advantages. [9] For such purposes one would need photonic so called GHZ (Greenberger-Horne-Zeilinger) states, which are states of mutually entangled qubits on the form presented in equation 7. [9] [2]

$$|\Psi\rangle = \frac{1}{\sqrt{2}}\left(|0\rangle^{\otimes N} + |1\rangle^{\otimes N}\right) \tag{7}$$

For quantum computers such as these one would need three-photon GHZ states, i.e. $N = 3$ in equation 7. [9]

### 2.4 Motivation

This brief account of quantum information is of course very far from a complete description of the field of research, nor does it mention all the problems, advantages, possibilities or quirks of this vast subject. However, it hopefully does serve as a sufficient motivation for the production of entangled photonic cluster states, which will be the object of investigation for the remaining part of this thesis.

## 3 The Protocol

The aim of the protocol described in this section, is to produce a states of entangled photons. This is done by shining pulsed laser light on a three-level quantum system, which has energy levels $|1\rangle$, $|2\rangle$ and $|0\rangle$, thereby causing excitation and latter spontaneous decay thereby emitting photons. The laser light used is assumed to be monochromatic, and is made to be resonant with the $|1\rangle - |2\rangle$ transition. The system is shown in figure 2.

The protocol is described in both [8] and [10]. It produces photons in a GHZ entangled state in the basis of time bins, and is described in the following steps:

1. The system begins in a state $|\Psi\rangle$, which is a superposition of states $|0\rangle$ and $|1\rangle$. By absorption of a $\pi$-pulse resonant with the $|1\rangle$-$|2\rangle$ transition, it becomes a superposition of $|0\rangle$ and $|2\rangle$. After spontaneous emission,

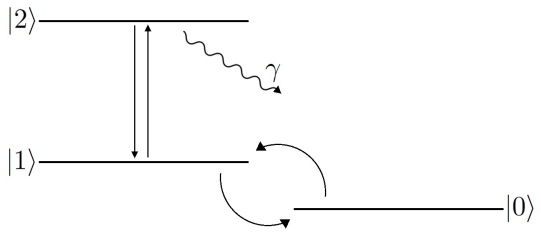


Figure 2: Schematics of the three-level quantum systems which is used in the protocol. The possible transition are marked by arrows.

the system will be in a superposition of $|0\rangle$ and $|1\rangle$ with an emitted photon. As this photon is emitted in the first part of the protocol, it is in an early time bin, and is thus denoted $e_1$.

$$\frac{1}{\sqrt{2}}(|0\rangle + |1\rangle) \rightarrow \frac{1}{\sqrt{2}}(|0\rangle + |2\rangle) \rightarrow \frac{1}{\sqrt{2}}(|0\rangle + |e_1,\, 1\rangle) \tag{8}$$

2. A population inversion is made using a $\pi$-pulse resonant with the $|0\rangle$-$|1\rangle$ transition.

$$\frac{1}{\sqrt{2}}(|0\rangle + |e_1,\, 1\rangle) \rightarrow \frac{1}{\sqrt{2}}\left(|1\rangle - |e_1, 0\rangle\right) \tag{9}$$

3. The excitation by absorption of laser light is repeated, thereby causing a superposition between the electron now being in $|0\rangle$ with the earlier emitted photon, or the electron now being in $|1\rangle$ with the spontaneous emission of a photon, which is said to be in the late time bin and is denoted, $L_1$.

$$\frac{1}{\sqrt{2}}\left(|1\rangle - |e_1, 0\rangle\right) \rightarrow \frac{1}{\sqrt{2}}\left(|2\rangle - |e_1, 0\rangle\right) \rightarrow \frac{1}{\sqrt{2}}\left(|L_1, 1\rangle - |e_1, 0\rangle\right) \tag{10}$$

4. The population inversion is repeated and the system returns to the original superposition with, however, a minus sign and an emitted photon in a superposition of early and late time bins.

$$\frac{1}{\sqrt{2}}\left(|L_1, 1\rangle - |e_1, 0\rangle\right) \rightarrow -\frac{1}{\sqrt{2}}\left(|L_1, 0\rangle + |e_1, 1\rangle\right) \equiv M|\Psi\rangle \tag{11}$$

By applying this protocol $N$ times, one will end up having a state described by equation 13.

$$(M)^N|\Psi\rangle = \frac{(-1)^N}{\sqrt{2}}\left(|L1, L_2, ..., L_N, 0\rangle + |e_1, e_2, ..., e_N, 1\rangle\right) \tag{12}$$

$$= \frac{(-1)^N}{\sqrt{2}}\left(|L\rangle^{\otimes N}|0\rangle + |e\rangle^{\otimes N}|1\rangle\right) \tag{13}$$

Upon measurement of the time bin, the photons will either be found to be in the early time bin, corresponding to the system being in $|1\rangle$, or in the late time bin, corresponding to the system being in $|0\rangle$. The state in equation 13 is therefore a state of $N$ entangled photon, as the measurement of one being in either the early or the late time been will result in all the other photons being in this time bin as well. Each of these two outcomes has a probability of $\frac{1}{2}$, and thus the entangled state is a GHZ state, which is what is wanted in quantum computation.

If a $\frac{\pi}{2}$-pulse instead of a $\pi$-pulse had been used to drive the transitions, one would have a more complicated superposition state as one would not make the complete population inversions that is the result of a $\pi$-pulse. This more complicated entangled state would be a cluster state. Thus the protocol can be used to create cluster states with only a slight alteration, and the description of the system will therefore be relevant for the understanding of the production of cluster states.

### 3.1 A far-detuned transistion

In reality one would not have an ideal three-level system. For instance there could be another level in the system, which will here be denoted $|3\rangle$. The transition between $|0\rangle$ and $|3\rangle$ is far-detuned to the laser light with a difference in frequency of $\Delta$. This is shown in figure 3. It is supposed that the system can be constructed to have selection rules, that ensure that no cross terms are possible, i.e. no transitions $|1\rangle$-$|3\rangle$ or $|0\rangle$-$|2\rangle$ can occur.

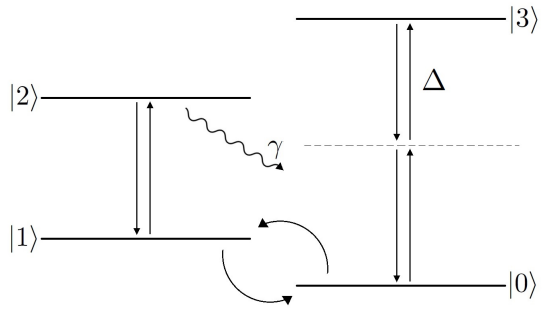


Figure 3: Schematics of the quantum system where transitions to a fourth level with detuning $\Delta$ is possible.

Though the transition $|0\rangle$-$|3\rangle$ is not at resonance with the laser light, it is possible to cause excitations from $|0\rangle$ to $|3\rangle$ if the laser pulse is sufficiently short. This is because of the integral of the intensity over time is fixed to be $\pi$, meaning that a shorter pulse length results in a narrower and therefore higher peak. A short pulse will thus have a much larger intensity, which raises the probability of excitations to the far-detuned level. This means that the pulse will drive both transitions and the crate the following states.

$$|1\rangle \rightarrow c_1|1\rangle + c_2|2\rangle \tag{14}$$

$$|0\rangle \rightarrow c_0|0\rangle + c_3|3\rangle \tag{15}$$

When going through the protocol one only wants to drive the resonant $|1\rangle$-$|2\rangle$ transition and not the far-detuned $|0\rangle$-$|3\rangle$ transition. In order to do this, it is useful to work with a concept known as fidelity, $F$, which describes how close two quantum states, $|\lambda\rangle$ and $|\phi\rangle$, are. It is defines as the squared overlap between the wave functions as shown in equation 16.

$$F = |\langle\lambda|\phi\rangle|^2 \tag{16}$$

At the end of the pulse one wants the resonant transition to be in the excited state, whereas the far-detuned transition is in the ground state. To maximise the probability of this corresponds to maximising the fidelity of these two states, which is equal to the expression in equation 17.

$$F = |c_2|^2|c_0|^2 \tag{17}$$

The goal is thus to find the pulse length, $T$, which maximises the expression in equation 16. This illustrates how the laser needs to be shone on the system for a sufficiently long time in order not to excite the far-detuned transistion, while, if the laser is operating for too long, the resonant system may have time to decay spontaneously, be re-excited and thus end up emitting two photons rather than the one that is needed for the protocol. The pulse length which maximises the fidelity, will be the one which is niether too long, such that spontaneous decay of the resonant transition is probable, nor too short, such that excitations to the far-detuned level is probable. The next step is therefore to calculate the coefficients $c_1(T)$, $c_2(T)$, $c_0(T)$ and $c_3(T)$ in order to be able to calculate the fidelity.

## 4 Equations describing the Coefficients

Because of the spontaneous emission from $|2\rangle$ to $|1\rangle$ and the excitation of $|0\rangle$ to $|3\rangle$, that one needs to take into account, the coefficients cannot be calculated analytically. Theses two issues can, however, be treated as perturbations to a system with no spontaneous emission and no excitations from $|0\rangle$. As no cross terms are

possible, the system can be treated as two separate two-level systems; one resonant and one far-detuned. The calculations done in this sections follows the method of [10].

The laser is described by a Gaussian pulse and the calculations are done semi-classically, meaning that the two-level system is treated quantum mechanically and the laser classically. Thus one has the quantum mechanical ground level $|g\rangle$ and excited level $|e\rangle$ with difference in energy $\hbar\,\omega_0$ illuminated by classical, monochromatic electromagnetic field, given in equation 18.

$$\overline{E} = \frac{\overline{\epsilon}(\overline{r},t)}{2}\mathrm{e}^{-i(\nu t-\overline{k}\overline{r})} + \frac{\overline{\epsilon}(\overline{r},t)^*}{2}\mathrm{e}^{i(\nu t-\overline{k}\overline{r})} \tag{18}$$

It is assumed that $\epsilon$ varies at much larger time scales than the optical frequency $\nu$ and much larger length scales than the optical length $\overline{k}$. In presence of a static electrical field, neutral atoms, or quantum dots, get a dipole moment $\hat{d}$ that interact with $\overline{E}$, and gives energy $\hat{U} = -\hat{d}\overline{E}$. The dipole operator is given by the following when, due to selection rules, the transitions are only between two energy levels.

$$\hat{d} = |g\rangle\langle e|\mu_{ge} + |e\rangle\langle g|\mu_{eg} \tag{19}$$

Here $\mu_{ge} = \langle g|\hat{d}|e\rangle$ and $\langle g|\hat{d}|g\rangle = \langle e|\hat{d}|e\rangle = 0$ meaning that there is no associated permanent dipole. [10] The Hamiltonian is given as the energy of the levels, 0 for $|g\rangle$ and $\omega$ for $|e\rangle$ (as only the difference in energy matters), plus the potential given by the field. The definitions $\sigma_{ge} = |g\rangle\langle e|$ and $\sigma_{eg} = |e\rangle\langle g|$ are used in the expression of the Hamiltonian in equation 20.

$$\hat{H} = \omega_0|e\rangle\langle e| + \left(-\hat{d}\overline{E}\right) = \omega_0|e\rangle\langle e| - (\sigma_{ge}\mu_{ge} + \sigma_{eg}\mu_{eg})\left(\frac{\overline{\epsilon}}{2}\mathrm{e}^{-i\nu t} + \frac{\overline{\epsilon}^*}{2}\mathrm{e}^{i\nu t}\right) \tag{20}$$

It is proposed that $|\Psi\rangle = c_g|g\rangle + c_e|e\rangle$. The Schrödinger equation $i\dot{\Psi} = \hat{H}\Psi$ [11] is multiplied with $\langle e|$ on both sides.

$$i\langle e|\frac{d}{dt}|\Psi\rangle = \langle e|\hat{H}|\Psi\rangle \tag{21}$$

$$\Rightarrow i\dot{c}_g\langle e|g\rangle + i\dot{c}_e\langle e|e\rangle = \omega_0\, c_g\langle e|e\rangle\langle e|g\rangle + \omega_0\, c_e\langle e|e\rangle\langle e|e\rangle - \Big(\mu_{ge}\, c_g\langle e|g\rangle\langle e|g\rangle \tag{22}$$

$$+ \mu_{ge}\, c_e\langle e|e\rangle\langle g|e\rangle + \mu_{eg}\, c_g\langle e|e\rangle\langle g|g\rangle + \mu_{eg}\, c_e\langle e|e\rangle\langle g|e\rangle\Big)\left(\frac{\overline{\epsilon}}{2}\mathrm{e}^{-i\nu t} + \frac{\overline{\epsilon}^*}{2}\mathrm{e}^{i\nu t}\right)$$

$$\Rightarrow \dot{c}_e = -i\omega_0\, c_e + i\mu_{eg}\, c_g\left(\frac{\overline{\epsilon}}{2}\mathrm{e}^{-i\nu t} + \frac{\overline{\epsilon}^*}{2}\mathrm{e}^{i\nu t}\right) \tag{23}$$

And it is multiplied with $|g\rangle$ instead to give $\dot{c}_g$.

$$i\langle g|\frac{d}{dt}|\Psi\rangle = \langle g|\hat{H}|\Psi\rangle \tag{24}$$

$$\Rightarrow i\dot{c}_g\langle g|g\rangle + i\dot{c}_e\langle g|e\rangle = \omega_0\, c_g\langle g|e\rangle\langle e|g\rangle + \omega_0\, c_e\langle g|e\rangle\langle e|e\rangle - \Big(\mu_{ge}\, c_g\langle g|g\rangle\langle e|g\rangle \tag{25}$$

$$+ \mu_{ge}\, c_e\langle g|g\rangle\langle e|e\rangle + \mu_{eg}\, c_g\langle g|e\rangle\langle e|g\rangle + \mu_{eg}\, c_e\langle g|e\rangle\langle g|e\rangle\Big)\left(\frac{\overline{\epsilon}}{2}\mathrm{e}^{-i\nu t} + \frac{\overline{\epsilon}^*}{2}\mathrm{e}^{i\nu t}\right) \tag{26}$$

$$\Rightarrow \dot{c}_g = i\mu_{ge}\, c_e\left(\frac{\overline{\epsilon}}{2}\mathrm{e}^{-i\nu t} + \frac{\overline{\epsilon}^*}{2}\mathrm{e}^{i\nu t}\right) \tag{27}$$

A transformation $c_e(t) = \tilde{c_e}(t)\mathrm{e}^{-i\nu t}$, corresponding to rotating the frame, is made. In this way one will be able to

spot fast oscillating and slow oscillating terms.

$$\frac{d}{dt}\left(\tilde{c_e}\mathrm{e}^{-i\nu t}\right) = -i\omega_0\,\tilde{c_e}\mathrm{e}^{-i\nu t} + i\mu_{eg}\,c_g\left(\frac{\overline{\epsilon}}{2}\mathrm{e}^{-i\nu t} + \frac{\overline{\epsilon}^*}{2}\mathrm{e}^{i\nu t}\right) \tag{28}$$

$$\Rightarrow \dot{\tilde{c}}_e\mathrm{e}^{-i\nu t} = -i(\omega_0-\nu)\,\tilde{c_e}\mathrm{e}^{-i\nu t} + i\mu_{eg}\,c_g\left(\frac{\overline{\epsilon}}{2}\mathrm{e}^{-i\nu t} + \frac{\overline{\epsilon}^*}{2}\mathrm{e}^{i\nu t}\right) \tag{29}$$

$$\Rightarrow \dot{\tilde{c}}_e = -i\Delta\tilde{c_e} + i\mu_{eg}\,c_g\left(\frac{\overline{\epsilon}}{2} + \frac{\overline{\epsilon}^*}{2}\mathrm{e}^{2i\nu t}\right) \tag{30}$$

and

$$\dot{c}_g = i\mu_{ge}\,\tilde{c_e}\left(\frac{\overline{\epsilon}}{2}\mathrm{e}^{-2i\nu t} + \frac{\overline{\epsilon}^*}{2}\right) \tag{31}$$

Here $\Delta = \omega_0 - \nu$ is the detuning of the energy difference to the electromagnetic field. The relevant dynamics occur at frequencies proportional to $\Omega = \frac{\overline{\epsilon}\mu_{eg}}{\hbar}$, where $\Omega$ is the Rabi frequency [4]. Terms $\mathrm{e}^{2i\nu t}$ are neglected as $\Delta << \nu, \omega_0$ and $\Omega << \nu$ is assumed. This is done because the terms with $\mathrm{e}^{2i\nu t}$ oscillates a lot faster than the other, and thus they average out on the time scales relevant for the other terms. This is the rotating wave approximation. [4] It is used to reduce the equations to the form in equation 32.

$$\dot{\tilde{c}}_e = -\Delta\tilde{c_e} + i\frac{\Omega}{2}c_g \quad \text{and} \quad \dot{c}_g = i\frac{\Omega^*}{2}\tilde{c}_e \tag{32}$$

Here there is no spontaneous emission, as it arises from quantum effects which are not a part of this classical description of the field. [10] Spontaneous emission is included by adding $-\frac{\gamma}{2}c_e$, where $\gamma$ is the decay factor, to $\dot{c}_e$. The tilde over the coefficient is omitted and a change of variables, $\tau = \gamma t$, is made. Here $\tilde{\Delta} = \frac{\Delta}{\gamma}$ and $\tilde{\Omega} = \frac{\Omega}{\gamma}$ and $\tilde{\gamma} = \frac{\gamma}{\gamma} = 1$. This is a change to dimensionless coordinates, where everything is scaled with respect to $\gamma$. Henceforth everything will be expressed in dimensionless coordinates.

$$\dot{c}_e(\tau) = -\left(i\tilde{\Delta} + \frac{1}{2}\right)c_e(\tau) + i\frac{\tilde{\Omega}}{2}c_g(\tau) \quad \text{and} \quad \dot{c}_g(\tau) = i\frac{\tilde{\Omega}^*}{2}c_e(\tau) \tag{33}$$

Using equation 33 the equations of motion for the resonant system, where there is no detuning but is spontaneous emission, and for the far-detuned system, where there is no spontaneous emission, is found. These are the equation that needs to be solved in order to find expression for the coefficients.

$$\text{Far-detuned transition: } \dot{c_3}(\tau) = -i\tilde{\Delta}c_3(\tau) + i\frac{\tilde{\Omega}_3(\tau)_3}{2}c_0(\tau) \tag{34}$$

$$\dot{c_0}(\tau) = i\frac{\tilde{\Omega}_3(\tau)_3^*}{2}c_3(\tau) \tag{35}$$

$$\text{Resonant transition: } \dot{c_2}(\tau) = i\frac{\tilde{\Omega}_2(\tau)_2}{2}c_1(\tau) - \frac{1}{2}c_2(\tau) \tag{36}$$

$$\dot{c_1}(\tau) = i\frac{\tilde{\Omega}_2(\tau)_2^*}{2}c_2(\tau) \tag{37}$$

These cannot be solved exactly as the Rabi frequency, $\Omega$, depends on time. The Rabi frequency, i.e. the frequency of the oscillations of the populations [4], is defined as the dipole moment multiplied with the electric field, and is therefore, for the Gaussian pulse, given by equation 38, where $\alpha$ is a normalisation constant. The same laser drives both the resonant and the far-detuned transistions and therefore the electric field is the same. However, the dipole moment for the transitions can be different, and this is described by a factor $R = \frac{|\tilde{\Omega}_3|}{|\tilde{\Omega}_2|}$. In this thesis it is supposed that $R = 1$, and therefore that the Rabi frequencies are the same for both the resonant and the far-detuned transition. Later supposed that it is real, i.e. $\tilde{\Omega} = \tilde{\Omega}^* = |\tilde{\Omega}|$, though the calculations are done more generally, allowing for a complex $\tilde{\Omega}$.

$$|\tilde{\Omega}(\tau)| = \frac{\alpha}{\sqrt{2\pi}\sigma}\,\mathrm{e}^{-\left(\frac{\tau-\mu}{\sqrt{2}\sigma}\right)^2} \tag{38}$$

The Gaussian function describing the pulse is cut off in both ends at equal distances from the mean value, $\mu$, thereby giving it a length that is equal to $\beta$ times the standard deviation, $\sigma$. As this describes a laser that begins to shine upon the system at $\tau = 0$ and ends at $\tau = T$, the mean value is given by $\mu = \frac{T}{2}$ and the standard deviation by $\sigma = \frac{T}{\beta}$. If $\beta << 1$ the Gaussian is cut of close to it's maximum and thus resembles a square pulse. It is the aim of this project to look at the case of a Gaussian pulse which is why $\beta >> 1$ is used. [10]

As $\tilde{\Omega}$ describes a $\pi$-pulse, the integral over time must be equal to $\pi$.[4] By calculating this integral, the value of $\alpha$ can be found.

$$\pi = \int_0^T |\tilde{\Omega}(\tau)| d\tau = \int_0^T \frac{\alpha}{\sqrt{2\pi}\sigma} \mathrm{e}^{-\left(\frac{\tau-\mu}{\sqrt{2}\sigma}\right)^2} d\tau = \alpha \,\mathrm{erf}\left(\frac{T\sqrt{2}}{4\sigma}\right) = \alpha \,\mathrm{erf}\left(\frac{\beta\sqrt{2}}{4}\right) \tag{39}$$

$$\Rightarrow \alpha = \pi \left(\mathrm{erf}\left(\frac{\beta\sqrt{2}}{4}\right)\right)^{-1} \approx \pi \left(1 - \frac{\mathrm{e}^{\frac{-\beta^2}{8}}}{\sqrt{\pi}\beta} 2\sqrt{2}\right)^{-1} \approx \pi \tag{40}$$

Here the first approximation is a first order series expansion of the error function around $\beta = \infty$. Both this and the second approximation therefore works in the regime where $\beta >> 1$, which is what is used in the description of the Gaussian pulse.

# 5 Calculating the Coefficients

As the differential equations describing the coefficients cannot be solved analytically, perturbation theory [11] is used. Here the equations are expanded so that the zeroth order corresponds to the system without the presence of spontaneous decay and far-detuned transitions respectively, and the higher orders describe different orders of pertubations of the zeroth order caused by these effect. In this project, the differential equations are solved using first order pertubation theory, meaning that only the zeroth and first order terms of the expansion are calculated, and thus only the first order contribution of spontaneous decays and far-detuned transitions are taken into account.

For the solutions of the equations for the resonant transition, the reader is referred to [10]. In order to obtain the expressions for the coefficients of far-detuned two-level system equations 34 and 35 needs to be solved. These are first solved numerically, and the result of this is shown in figure 4. It is apparent how for very short pulses, that is small values of $\sigma$, the probability of the system being in the excited level $|3\rangle$ is very large, as $|c_3|^2$ is close to one and $|c_0|^2$ close to zero. As the pulse becomes longer, the probability of being in $|3\rangle$ drops towards zero. On the plot with the logarithmic scale on the vertical axis, it can be seen how $|c_3|^2$ eventually flattens out with only small jumps up and down caused by numerical error.

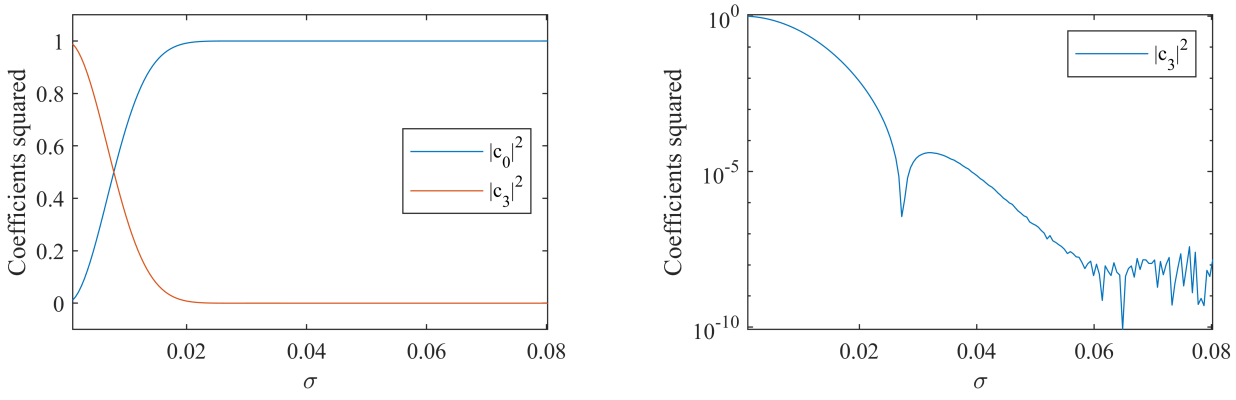


(a) on linear axes

(b) on semi-logarithmic axes

Figure 4: The numerical solutions of the differential equations as a function of different pulse widths $\sigma$ with $\beta = 10$ and $\tilde{\Delta} = 100$.

For the analytical solution to the equations, a change of variables to $\xi = |\tilde{\Omega}|\tau \Rightarrow d\xi = |\tilde{\Omega}_3|\, d\tau$ is made in

equations 34 and 35.

$$\dot{c_3}(\xi) = -i\frac{\tilde{\Delta}}{|\tilde{\Omega}_3|}c_3(\xi) + i\frac{\tilde{\Omega}_3}{2\,|\tilde{\Omega}_3|}c_0(\xi) \quad \text{and} \quad \dot{c_0}(\xi) = i\frac{\tilde{\Omega}_3^*}{2\,|\tilde{\Omega}_3|}c_3(\xi) \tag{41}$$

Perturbation is done with an expansion around $\epsilon = i\frac{\tilde{\Omega}_3}{2\,|\tilde{\Omega}_3|}$.

$$c_3(\xi) = c_3^{(0)}(\xi) + \epsilon\, c_3^{(1)}(\xi) + \epsilon^2 c_3^{(2)}(\xi) + ... \tag{42}$$

$$c_0(\xi) = c_0^{(0)}(\xi) + \epsilon\, c_0^{(1)}(\xi) + \epsilon^2 c_0^{(2)}(\xi) + ... \tag{43}$$

The expansions in equations 42 and 43 are inserted into the differential equations in equation 41 and collected in different orders of $\epsilon$.

$$\dot{c_3}^{(0)}(\xi) + \epsilon\,\dot{c_3}^{(1)}(\xi) + ... = -i\frac{\tilde{\Delta}}{|\tilde{\Omega}_3|}\left(c_3^{(0)}(\xi) + \epsilon\, c_3^{(1)}(\xi) + ...\right) + \epsilon\left(c_0^{(0)}(\xi) + \epsilon\, c_0^{(1)}(\xi) + ...\right) \tag{44}$$

$$\Rightarrow \text{Terms with order of } \epsilon^N: \quad \dot{c_3}^{(N)}(\xi) = -i\frac{\tilde{\Delta}}{|\tilde{\Omega}_3|}c_3^{(N)}(\xi) + c_0^{(N-1)}(\xi) \tag{45}$$

$$\dot{c_0}^{(0)}(\xi) + \epsilon\,\dot{c_0}^{(1)}(\xi) + ... = i\frac{\tilde{\Omega}_3^*}{2\,|\tilde{\Omega}_3|}\left(c_3^{(0)}(\xi) + \epsilon\, c_3^{(1)}(\xi) + ...\right) \tag{46}$$

$$= \frac{\tilde{\Omega}_3^{*2}}{|\tilde{\Omega}_3|^2}\epsilon\left(c_3^{(0)}(\xi) + \epsilon\, c_3^{(1)}(\xi) + \epsilon^2 c_3^{(2)}(\xi) + ...\right) \tag{47}$$

$$\Rightarrow \text{Terms with order of } \epsilon^N: \quad \dot{c_0}^{(N)}(\xi) = \frac{\tilde{\Omega}_3^{*2}}{|\tilde{\Omega}_3|^2}c_3^{(N-1)}(\xi) \tag{48}$$

There zeroth order equations are therefore the following.

$$\dot{c_3}^{(0)}(\xi) = -\frac{\tilde{\Delta}}{|\tilde{\Omega}_3|}c_3^{(0)}(\xi) \quad \text{and} \quad \dot{c_0}^{(0)}(\xi) = 0 \tag{49}$$

The initial conditions are $c_0^{(0)}(0) = 1$ and $c_3^{(0)}(0) = 0$. As $\dot{c_0}^{(0)}(\xi) = 0$ it means that $c_0^{(0)}$ is constant and thus $c_0^{(0)}(\xi) = 1$, which means that $c_3^{(0)}(\xi) = 0$ because of normalisation. Thus there are no transition to the far-detuned level up to the zeroth order.

By setting $N = 1$ one obtains the first order equations.

$$\dot{c_3}^{(1)}(\xi) = -i\frac{\tilde{\Delta}}{|\tilde{\Omega}_3|}c_3^{(1)}(\xi) + c_0^{(0)}(\xi) = -i\frac{\tilde{\Delta}}{|\tilde{\Omega}_3|}c_3^{(1)}(\xi) + 1 \tag{50}$$

$$\dot{c_0}^{(1)}(\xi) = \frac{\tilde{\Omega}_3^{*2}}{|\tilde{\Omega}_3|^2}c_3^{(0)}(\xi) = 0 \tag{51}$$

At $\tau = 0$ there is no excitation to the far-detuned level yet and thus no correction the the zeroth order. The initial conditions are therefor $c_3^{(1)}(0) = c_0^{(1)}(0) = 0$, and therefore $\dot{c_0}^{(1)}(\xi) = 0 \Rightarrow c_0^{(1)}(\xi) = 0$. The other equation is on the form of an inhomogeneous differential equation, and is solved by the method of Variation of Parameters. [3] This involves first solving the homogeneous version of the equation which is presented in equation 52

$$\dot{c_3}^{(1)}(\xi) + i\frac{\tilde{\Delta}}{|\tilde{\Omega}_3|^2}c_3^{(1)}(\xi) = 0 \tag{52}$$

The solution to a differential equation on the form $\dot{y} + p(x)\,y = 0$ is on the form $y = A\,\mathrm{e}^{-\int p(x)dx}$, where $A$ is a constant, as this will result in $\dot{y} = -p(x)\,y$. The solution to the homogeneous equation, called the complementary solution and thus denoted with a subscript $c$, is therefore as follows.

$$c_{3,c}^{(1)}(\xi) = A\,\mathrm{e}^{-i\int \frac{\tilde{\Delta}}{|\tilde{\Omega}_3|^2}d\xi'} \tag{53}$$

The particular solution to the inhomogeneous equation, denoted by subscript $p$, is then found by varying the constant $A$ in $\xi$.

$$c_{3,c}^{(1)}(\xi) = A(\xi)\,\mathrm{e}^{-i\int \frac{\tilde{\Delta}}{|\tilde{\Omega}_3|^2}d\xi'} \tag{54}$$

This expression is substituted into equation 50.

$$\dot{A}(\xi)\,\mathrm{e}^{-i\int \frac{\tilde{\Delta}}{|\tilde{\Omega}_3|^2}d\xi'} - i\frac{\tilde{\Delta}}{|\tilde{\Omega}_3|^2}\mathrm{e}^{-i\int \frac{\tilde{\Delta}}{|\tilde{\Omega}_3|^2}d\xi'} + i\frac{\tilde{\Delta}}{|\tilde{\Omega}_3|}A(\xi)\mathrm{e}^{-i\int \frac{\tilde{\Delta}}{|\tilde{\Omega}_3|^2}d\xi'} = 1 \tag{55}$$

$$\Rightarrow \dot{A}(\xi) = \mathrm{e}^{i\int \frac{\tilde{\Delta}}{|\tilde{\Omega}_3|^2}d\xi'} \Rightarrow A = \int \mathrm{e}^{i\int \frac{\tilde{\Delta}}{|\tilde{\Omega}_3|^2}d\xi'}d\xi' \tag{56}$$

Now that $A(\xi)$ has been found the full solution can be written.

$$c_3^{(1)}(\xi) = \mathrm{e}^{-i\int \frac{\tilde{\Delta}}{|\tilde{\Omega}_3|^2}d\xi'}\int \mathrm{e}^{i\int \frac{\tilde{\Delta}}{|\tilde{\Omega}_3|^2}d\xi'}d\xi' \tag{57}$$

The variables are then changed back to $\tau$.

$$\Rightarrow c_3^{(1)}(\tau) = \mathrm{e}^{-i\int_0^T \tilde{\Delta}d\tau'}\int_0^T \mathrm{e}^{i\int_0^{\tau'}\tilde{\Delta}\,d\tau''}|\tilde{\Omega}_3|\,d\tau' = \mathrm{e}^{-i\tilde{\Delta}\,T}\int_0^T \mathrm{e}^{i\tilde{\Delta}\tau'}\,|\tilde{\Omega}_3|\,d\tau' \tag{58}$$

The definitions of $\Omega$, $\mu$ and $\sigma$ are then inserted.

$$c_3^{(1)}(\xi) = \frac{\alpha}{\sqrt{2\pi}\sigma}\mathrm{e}^{-i\tilde{\Delta}T}\int_0^T \mathrm{e}^{i\tilde{\Delta}\tau'}\mathrm{e}^{-\left(\frac{\tau'-\mu}{\sqrt{2}\sigma}\right)^2}d\tau' \tag{59}$$

This expression can be reduced by looking for a way to rewrite the expression within the integral and using the definitions $\mu = \frac{T}{2}$ and $\sigma = \frac{T}{\beta}$.

$$\mathrm{e}^{-\left(\frac{\tau-\mu}{\sqrt{2}\sigma} - i\frac{\tilde{\Delta}}{\sqrt{2}}\sigma\right)^2} = \mathrm{e}^{\left(\frac{\tau-\mu}{\sqrt{2}\sigma}\right)^2}\mathrm{e}^{-\frac{\tilde{\Delta}^2T^2}{2\beta^2}}\mathrm{e}^{-i\tau\tilde{\Delta}}\mathrm{e}^{i\frac{T}{2}\tilde{\Delta}} \tag{60}$$

$$\Rightarrow \mathrm{e}^{i\tilde{\Delta}\tau'}\mathrm{e}^{-\left(\frac{\tau'-\mu}{\sqrt{2}\sigma}\right)^2} = \mathrm{e}^{-\frac{\tilde{\Delta}^2T^2}{2\beta^2}}\mathrm{e}^{i\frac{T}{2}\tilde{\Delta}}\mathrm{e}^{-\left(\frac{\tau-\mu}{\sqrt{2}\sigma} - i\frac{\tilde{\Delta}}{\sqrt{2}}\sigma\right)^2} \tag{61}$$

Using this the equation becomes the following.

$$c_3^{(1)}(\xi) = \frac{\alpha}{\sqrt{2\pi}\sigma}\mathrm{e}^{-i\frac{T\tilde{\Delta}}{2}}\mathrm{e}^{-\frac{\tilde{\Delta}^2T^2}{2\beta^2}}\int_0^T \mathrm{e}^{-\left(\frac{\tau-\mu}{\sqrt{2}\sigma} - i\frac{\tilde{\Delta}}{\sqrt{2}}\sigma\right)^2}d\tau' \tag{62}$$

Then a change of variables is made $u(\tau) = \frac{\tau-\mu}{\sqrt{2}\sigma} - i\frac{\tilde{\Delta}}{\sqrt{2}}\sigma \Rightarrow \frac{du}{d\tau} = \frac{1}{\sqrt{2}\sigma} \Rightarrow d\tau = \sqrt{2}\sigma\,du$.

$$c_3^{(1)}(\xi) = \frac{\alpha}{\sqrt{\pi}}\mathrm{e}^{-i\frac{T\tilde{\Delta}}{2}}\mathrm{e}^{-\frac{\tilde{\Delta}^2T^2}{2\beta^2}}\int_{u(0)}^{u(T)} \mathrm{e}^{-u^2}du \tag{63}$$

$$= \frac{\alpha}{\sqrt{\pi}}\mathrm{e}^{-i\frac{T\tilde{\Delta}}{2}}\mathrm{e}^{-\frac{\tilde{\Delta}^2T^2}{2\beta^2}}\left(\int_0^{u(T)} \mathrm{e}^{-u^2}du - \int_0^{u(0)} \mathrm{e}^{-u^2}du\right) \tag{64}$$

$$= \frac{\alpha}{\sqrt{\pi}}\mathrm{e}^{-i\frac{T\tilde{\Delta}}{2}}\mathrm{e}^{-\frac{\tilde{\Delta}^2T^2}{2\beta^2}}\left(\frac{\sqrt{\pi}}{2}\mathrm{erf}\left(u(T)\right) - \frac{\sqrt{\pi}}{2}\mathrm{erf}\left(u(0)\right)\right) \tag{65}$$

$$= \frac{\alpha}{2}\mathrm{e}^{-i\frac{T\tilde{\Delta}}{2}}\mathrm{e}^{-\frac{\tilde{\Delta}^2T^2}{2\beta^2}}\left(\mathrm{erf}\left(\frac{T-\mu}{\sqrt{2}\sigma} - i\frac{\tilde{\Delta}}{\sqrt{2}}\sigma\right) + \mathrm{erf}\left(\frac{\mu}{\sqrt{2}\sigma} + i\frac{\tilde{\Delta}}{\sqrt{2}}\sigma\right)\right) \tag{66}$$

$$= \frac{\alpha}{2}\mathrm{e}^{-i\frac{T\tilde{\Delta}}{2}}\mathrm{e}^{-\frac{\tilde{\Delta}^2T^2}{2\beta^2}}\left(\mathrm{erf}\left(\frac{\beta}{2\sqrt{2}} - i\frac{\tilde{\Delta}T}{\sqrt{2}\beta}\right) + \mathrm{erf}\left(\frac{\beta}{2\sqrt{2}} + i\frac{\tilde{\Delta}T}{\sqrt{2}\beta}\right)\right) \tag{67}$$

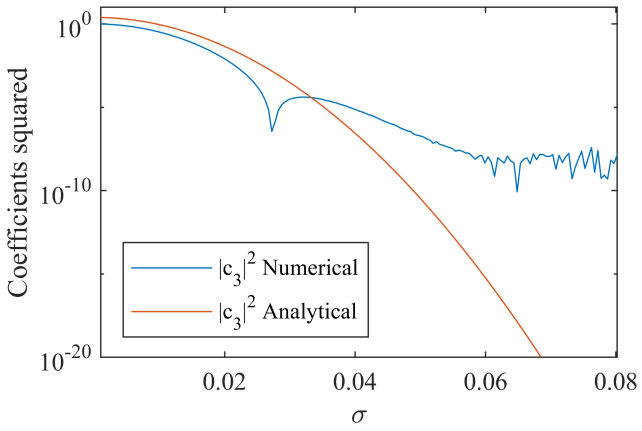


Figure 5: A plot of the numerical and analytical solutions to the differential equations describing $|c_0|^2$ and $|c_3|^2$ as function of the pulse width $\sigma$ for $\beta = 10$ and $\tilde{\Delta} = 100$.

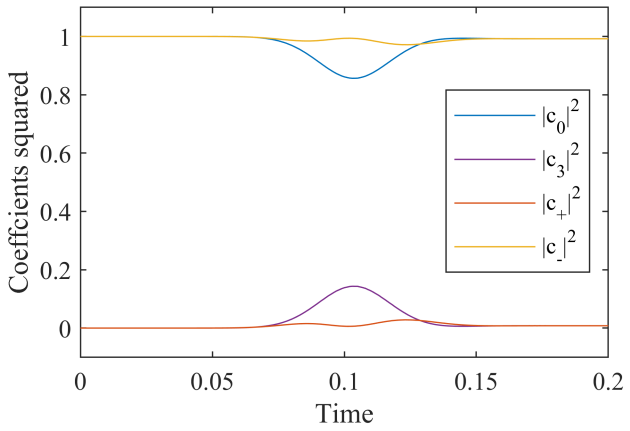


Figure 6: The numerical solutions for $|c_0|^2$ and $|c_3|^2$ together with projections of these into the basis dressed states, $|c_+|^2$ and $|c_-|^2$. Both as functions of the during a pulse with $\sigma = 0.02$ and with $\beta = 10$ and $\tilde{\Delta} = 100$

.

And as $\beta >> 1$ the term $\frac{\tilde{\Delta}T}{\sqrt{2}\beta} << 1$, which is inserted. The values of the normalization factor, $\alpha = \pi \left(\text{erf}\left(\frac{\beta}{2\sqrt{2}}\right)\right)^{-1}$, is also used.

$$c_3^{(1)}(\xi) \approx \alpha\, \mathrm{e}^{-i\frac{T\tilde{\Delta}}{2}} \mathrm{e}^{-\frac{\tilde{\Delta}^2T^2}{2\beta^2}} \text{erf}\left(\frac{\beta}{2\sqrt{2}}\right) \approx \pi\, \mathrm{e}^{-i\frac{T\tilde{\Delta}}{2}} \mathrm{e}^{-\frac{\tilde{\Delta}^2T^2}{2\beta^2}} \tag{68}$$

Now that both first order corrections have been found, the expressions for the coefficients can be written down up to the first order.

$$c_0(\xi) \simeq c_0^{(0)}(\xi) + \epsilon c_0^{(1)}(\xi) = 1 + \epsilon \cdot 0 = 1 \tag{69}$$

$$c_3(\xi) \simeq c_3^{(0)}(\xi) + \epsilon c_3^{(1)}(\xi) \approx 0 + \frac{i}{2}\frac{\tilde{\Omega}_3}{|\tilde{\Omega}_3|}\pi R\, \mathrm{e}^{-i\frac{T\tilde{\Delta}}{2}} \mathrm{e}^{-\frac{\tilde{\Delta}^2T^2}{2\beta^2}} \tag{70}$$

Finally the modulus square is calculated, as this is what is physically relevant.

$$|c_3|^2 = c_3\, c_3^* = \frac{i}{2}\frac{\tilde{\Omega}_3}{|\tilde{\Omega}_3|}\pi R\, \mathrm{e}^{-i\frac{T\tilde{\Delta}}{2}} \mathrm{e}^{-\frac{\tilde{\Delta}^2T^2}{2\beta^2}} \left(-\frac{i}{2}\frac{\tilde{\Omega}_3}{|\tilde{\Omega}_3^*|}\pi R\, \mathrm{e}^{i\frac{T\tilde{\Delta}}{2}} \mathrm{e}^{-\frac{\tilde{\Delta}^2T^2}{2\beta^2}}\right) = \frac{\pi^2}{4}\mathrm{e}^{-\frac{\tilde{\Delta}^2T^2}{\beta^2}} \tag{71}$$

$$|c_0|^2 = 1 - |c_3|^2 = 1 - \frac{\pi^2}{4}\mathrm{e}^{-\frac{\tilde{\Delta}^2T^2}{\beta^2}} \tag{72}$$

In order to determine whether this solution is good or not, the analytical result in equation 72 is compared with a numerical solution of the differential equation. This is done in figure 5, which showns that the analytical solution found by perturbation theory does not at all correspond to the numerical solution. An explanation for this is offered by looking at the numerically found coefficients as a function of the real time during a pulse, as shown in figure 6, where $|c_3|^2$ and $|c_0|^2$ have been plotted.

The perturbation is done with a zeroth order that describes a system with no excitations to the far-detuned level $|3\rangle$, which corresponds to doing it around values of $|c_0|^2 = 1$ and $|c_3|^2 = 0$. But as it appears in figure 6 this is far from being the case. It seems like the change in the coefficients due to far-detuned excitations are too great for perturbation theory to work. Thus another method must be thought of.

## 5.1 Dressed states

The states $|0\rangle$ and $|1\rangle$ used up untill now are called bare states. When working with for instance problems of light-atom interaction it is often worthwhile to describe the system in a basis of so called dressed states instead.

These are the eigenstates of the effective Hamiltonian of the system. [12] The equations of motion for this system, equations 34 and 35, can be viewed as resulting from the effective Hamiltonian shown in equation 73.

$$\hat{H}_{ef} = -\tilde{\Delta}|3\rangle\langle 3| - \left(\frac{\tilde{\Omega}}{2}|3\rangle\langle 0| + \frac{\tilde{\Omega}^*}{2}|0\rangle\langle 3|\right) \tag{73}$$

This is proven by inserting this Hamiltonian and a state $|\Psi\rangle = c_0|0\rangle + c_3|3\rangle$ into the Schrödinger equation [11] and multiplying with $\langle 3|$ from the left on both sides.

$$i\frac{d}{dt}|\Psi\rangle = \hat{H}_{ef}|\Psi\rangle \Rightarrow\ i\langle 3|\frac{d}{dt}|\Psi\rangle = \langle 3|\hat{H}_{ef}|\Psi\rangle \Rightarrow\ \dot{c_3} = i\tilde{\Delta}c_3 + i\frac{\tilde{\Omega}}{2}c_0 \tag{74}$$

And by multiplying with $\langle 0|$ from the left on both sides.

$$i\frac{d}{dt}|\Psi\rangle = \hat{H}_{ef}|\Psi\rangle \Rightarrow\ i\langle 0|\frac{d}{dt}|\Psi\rangle = \langle 0|\hat{H}_{ef}|\Psi\rangle \Rightarrow\ \dot{c_0} = i\frac{\tilde{\Omega}^*}{2}c_3 \tag{75}$$

This shows that by using this effective Hamiltonian the equations of motion (equations 34 and 35) are retrieved.

In the basis of $|0\rangle$ and $|3\rangle$ the effective Hamiltonian is given as in equation 76 on matrix form.

$$\hat{H}_{ef} = -\begin{pmatrix} 0 & \frac{\tilde{\Omega}^*}{2} \\ \frac{\tilde{\Omega}}{2} & \tilde{\Delta} \end{pmatrix} \tag{76}$$

This matrix can be diagonalized if written in the basis of its own eigenvector. The eigenvectors of the effective Hamiltonian is given in equations 77 and 78 and and the eigenvalue in equation 79. Here $\theta = \arctan\frac{\tilde{\Omega}}{\tilde{\Delta}}$ has been used.

$$|+\rangle = \cos\frac{\theta}{2}|0\rangle + \sin\frac{\theta}{2}|3\rangle \tag{77}$$

$$|-\rangle = \sin\frac{\theta}{2}|0\rangle - \cos\frac{\theta}{2}|3\rangle \tag{78}$$

$$\epsilon_\pm = \frac{1}{2}\left(-\tilde{\Delta} \mp \sqrt{\tilde{\Delta}^2 + 4|\tilde{\Omega}|^2}\right) \tag{79}$$

As can be seen these eigenstates remain the same, for rotations the Bloch vector (in the bare state basis), i.e. oscillations between the states $|0\rangle$ and $|1\rangle$. If the system remains in the same state, the Hamiltonian is constant. This means that the effective Hamiltonian is the Hamiltonian of the system seen from the rotating frame of $|+\rangle$ and $|-\rangle$. If the effective Hamiltonian is not exactly constant, but changes very slowly, the eigenstates are approximately stationary. This is known as the adiabatic limit. Here population fluctuations are therefore negligable, and the system is said to adiabatically follow one eigenstate. [12]

A special case of this, which is known as adiabatic return, is obtained when $\tilde{\Delta}$ is constant and not equal to zero. If the system then adiabatically follows $|-\rangle$ it will be in state $|0\rangle$ prior to the pulse, as $\tilde{\Omega} = 0$ meaning that $\theta = 0$ which gives coefficients $\cos\frac{\theta}{2} = 1$ and $\sin\frac{\theta}{2} = 0$. During the pulse the system will be in a superposition of states $|0\rangle$ and $|3\rangle$, but by the end of the pulse, when $\omega \to 0$, the system will return to $|0\rangle$. [12]

In figure 6 the dressed state coefficients are plotted. They have been found as a projection of the numerical solutions to the differential equations, as given by equation 80 and 81, which is in turn given by equations 77 and 78.

$$c_+(\tau) = \cos\frac{\theta}{2}c_0(\tau) + \sin\frac{\theta}{2}c_3(\tau) \tag{80}$$

$$c_-(\tau) = \sin\frac{\theta}{2}c_0(\tau) - \cos\frac{\theta}{2}c_3(\tau) \tag{81}$$

As can be seen in figure 6 these coefficients are much closer to being constantly 0 and 1 respectively during the pulse, and the system can be viewed as making an adiabatic return. It should therefore be advantageous to make

a perturbation around dressed states being stationary, i.e. around $|c_+|^2 = 1$ and $|c_-|^2 = 0$, rather than around the bare states being stationary. To do this, the equations of motion must be written in the basis of the dressed states.

An arbitrary state of the system can be written as in equation 82. [12]

$$|\psi(\tau)\rangle = \sum_l c_l(\tau) \mathrm{e}^{-i\int_0^t \epsilon_l(\tau')d\tau'} |l\rangle = c_+(\tau)\mathrm{e}^{-i\int_0^\tau \epsilon_+(\tau')d\tau'}|+\rangle + c_-(\tau)\mathrm{e}^{-i\int_0^\tau \epsilon_-(\tau')d\tau'}|-\rangle \tag{82}$$

This state is inserted intro the Schrödinger equation together with the effective Hamiltonian. Here the rule of differentiation $\frac{\partial}{\partial t}(f\,g\,h) = \frac{\partial f}{\partial t}\,g\,h + \frac{\partial g}{\partial t}\,h\,f + \frac{\partial h}{\partial t}\,f\,g$ is used.

$$\hat{H}_{ef}|\Psi\rangle = i\frac{\partial}{\partial t}|\Psi\rangle = i\sum_l \dot{c}_l(\tau)\mathrm{e}^{-i\int_0^\tau \epsilon_l d\tau'}|l\rangle + \sum_l \epsilon_l c_l(\tau)\mathrm{e}^{-i\int_0^\tau \epsilon_l d\tau'}|l\rangle + i\sum_l c_l(\tau)\mathrm{e}^{-i\int_0^\tau \epsilon_l d\tau'}\frac{\partial|l\rangle}{\partial\tau} \tag{83}$$

The time independent Schrödinger equation states that $\hat{H}|\Psi\rangle = E\,|\psi\rangle$ [11], which can be used on the left side of the equality sign.

$$\Rightarrow \sum_l \epsilon_l|\Psi\rangle = i\sum_l \dot{c}_l(\tau)\mathrm{e}^{-i\int_0^\tau \epsilon_l d\tau'}|l\rangle + \sum_l \epsilon_l|\Psi\rangle + i\sum_l c_l(\tau)\mathrm{e}^{-i\int_0^\tau \epsilon_l d\tau'}\frac{\partial|l\rangle}{\partial\tau} \tag{84}$$

$$\Rightarrow \sum_l \dot{c}_l(\tau)\mathrm{e}^{-i\int_0^\tau \epsilon_l d\tau'}|l\rangle = -\sum_l c_l(\tau)\mathrm{e}^{-i\int_0^\tau \epsilon_l d\tau'}\frac{\partial|l\rangle}{\partial\tau} \tag{85}$$

This expression is multiplied with $|n\rangle$ from the left on both sides. The dressed state are orthonormal, meaning that $\langle n|l\rangle = \delta_{n,l}$ [11], where $\delta_{n,l}$ is the Dirac $\delta$-function.

$$\sum_l \dot{c}_l(\tau)\mathrm{e}^{-i\int_0^\tau \epsilon_l d\tau'}\langle n|l\rangle = -\sum_l c_l(\tau)\mathrm{e}^{-i\int_0^\tau \epsilon_l d\tau'}\langle n|\frac{\partial}{\partial\tau}|l\rangle \tag{86}$$

$$\Rightarrow \dot{c}_n(\tau) = -\sum_l c_l(\tau)\,\mathrm{e}^{-i\int_0^\tau (\epsilon_l-\epsilon_n)d\tau'}\langle n|\frac{\partial}{\partial\tau}|l\rangle \tag{87}$$

It is thus necessary to calculate $\langle n|\frac{\partial}{\partial\tau}|l\rangle$ for the dressed states.

$$\langle+|\frac{\partial}{\partial\tau}|+\rangle = \left(\cos\frac{\theta}{2}\langle 0| + \sin\frac{\theta}{2}\langle 3|\right)\frac{\partial}{\partial\tau}\left(\cos\frac{\theta}{2}|0\rangle + \sin\frac{\theta}{2}|3\rangle\right) = 0 \tag{88}$$

$$\langle+|\frac{\partial}{\partial\tau}|-\rangle = \left(\cos\frac{\theta}{2}\langle 0| + \sin\frac{\theta}{2}\langle 3|\right)\frac{\partial}{\partial\tau}\left(\sin\frac{\theta}{2}|0\rangle - \cos\frac{\theta}{2}|3\rangle\right) = \frac{1}{2}\frac{\partial\theta}{\partial\tau} \tag{89}$$

$$\langle-|\frac{\partial}{\partial\tau}|-\rangle = \left(\sin\frac{\theta}{2}\langle 0| - \cos\frac{\theta}{2}\langle 3|\right)\frac{\partial}{\partial\tau}\left(\sin\frac{\theta}{2}|0\rangle - \cos\frac{\theta}{2}|3\rangle\right) = 0 \tag{90}$$

$$\langle-|\frac{\partial}{\partial\tau}|+\rangle = \left(\sin\frac{\theta}{2}\langle 0| - \cos\frac{\theta}{2}\langle 3|\right)\frac{\partial}{\partial\tau}\left(\cos\frac{\theta}{2}|0\rangle + \sin\frac{\theta}{2}|3\rangle\right) = -\frac{1}{2}\frac{\partial\theta}{\partial\tau} \tag{91}$$

These values are inserted into equation 87.

$$\dot{c}_- = -\mathrm{e}^{-i\int_0^\tau \epsilon_+-\epsilon_- d\tau'}\langle-|\frac{\partial}{\partial\tau}|+\rangle\,c_+ - \mathrm{e}^0\,\langle-|\frac{\partial}{\partial\tau}|-\rangle = \mathrm{e}^{-i\int_0^\tau \epsilon_+-\epsilon_- d\tau'}\frac{1}{2}\frac{\partial\theta}{\partial\tau} \tag{92}$$

$$\dot{c}_+ = -\mathrm{e}^{-i\int_0^\tau \epsilon_--\epsilon_+ d\tau'}\langle+|\frac{\partial}{\partial\tau}|-\rangle\,c_- - \mathrm{e}^0\,\langle+|\frac{\partial}{\partial\tau}|+\rangle = -\mathrm{e}^{-i\int_0^\tau \epsilon_+-\epsilon_- d\tau'}\frac{1}{2}\frac{\partial\theta}{\partial\tau} \tag{93}$$

The energy difference is then to be found.

$$\epsilon_+ - \epsilon_- = \frac{1}{2}\left(-\tilde{\Delta} + \sqrt{\tilde{\Delta}^2 + 4\tilde{\Omega}^2}\right) - \frac{1}{2}\left(-\tilde{\Delta} - \sqrt{\tilde{\Delta}^2 + 4\tilde{\Omega}^2}\right) = \sqrt{\tilde{\Delta}^2 + 4\tilde{\Omega}^2} \tag{94}$$

And the derivative of $\theta$, where it is used that $\Delta$ is constant.

$$\frac{\partial\theta}{\partial\tau} = \frac{\partial}{\partial\tau}\arctan\frac{\tilde{\Omega}}{\tilde{\Delta}} = \frac{1}{\left(\frac{\tilde{\Omega}}{\tilde{\Delta}}\right)^2 + 1}\frac{1}{\tilde{\Delta}}\frac{\partial\tilde{\Omega}}{\partial} = \frac{1}{\frac{\tilde{\Omega}^2}{\tilde{\Delta}} + \tilde{\Delta}}\frac{\partial\tilde{\Omega}}{\partial\tau} = \frac{\tilde{\Delta}}{\tilde{\Omega}^2 + \tilde{\Delta}^2}\frac{\partial\tilde{\Omega}}{\partial\tau} \tag{95}$$

The dericative of $\tilde{\Omega}$ is also calculated.

$$\frac{\partial\tilde{\Omega}}{\partial\tau} = \frac{\partial}{\partial\tau}\frac{\alpha}{\sqrt{2\pi}\sigma}\,\mathrm{e}^{-\left(\frac{\tau-\mu}{\sqrt{2}\sigma}\right)^2} = -\frac{\alpha}{\sqrt{2\pi}\sigma^3}(\tau-\mu)\,\mathrm{e}^{-\left(\frac{\tau-\mu}{\sqrt{2}\sigma}\right)^2} \tag{96}$$

By inserting all this into equations 92 and 93, the differential equations, which needs to be solved, are found.

$$\dot{c}_-(\tau) = -\frac{\alpha}{2\sqrt{2\pi}\sigma^3}\,\frac{\tilde{\Delta}}{\tilde{\Omega}^2+\tilde{\Delta}^2}\,(\tau-\mu)\,\mathrm{e}^{-i\int_0^\tau\sqrt{\tilde{\Omega}^2+\tilde{\Delta}^2}d\tau'}\,\mathrm{e}^{-\left(\frac{\tau-\mu}{\sqrt{2}\sigma}\right)^2}\,c_+(\tau) \tag{97}$$

$$\dot{c}_+(\tau) = \frac{\alpha}{2\sqrt{2\pi}\sigma^3}\,\frac{\tilde{\Delta}}{\tilde{\Omega}^2+\tilde{\Delta}^2}\,(\tau-\mu)\,\mathrm{e}^{i\int_0^\tau\sqrt{\tilde{\Omega}^2+\tilde{\Delta}^2}d\tau'}\,\mathrm{e}^{-\left(\frac{\tau-\mu}{\sqrt{2}\sigma}\right)^2}\,c_-(\tau) \tag{98}$$

Before beginning to solve this, it is reasonable to test whether moving to the dressed state basis is a problem. To this purpose the numerical solutions for $|c_3|^2$ and $|c_-|^2$ are compared in figure 7. The values at the end of the pulse, at $\tau = T$, of $c_-$ should correspond to the end values of $c_3$ as $\theta = 0$, and in figure 7 these endvalues are plotted for different pulses, i.e. different values of $\sigma$, and a comparison shows that the bare and dressed states do indeed match to a high degree. A shift to the dressed state picture should therefore not be a problem. The small difference, which is apparent at the very end, is due to the fact that the pulse is cut off at a distance $\frac{\sigma\beta}{2}$ from the maximum, which means that at the end of the pulse one does not exactly have $\cos\frac{\theta}{2} = 1$ and $\sin\frac{\theta}{2} = 0$, because $\tilde{\Omega}$, and therefore $\theta$, is not exactly zero. This is underlined by the graphs of the numerical solutions for both $|c_-|^2$ and $|c_3|^2$ where the value at the endpoints, $t = 0$ or $t = T$, have been subtracted from $\tilde{\Omega}$, so as to move the Gaussian function down. That is to say, in the differential equations $\tilde{\Omega}'(\tau) = \tilde{\Omega}(\tau) - \tilde{\Omega}(T)$ rather than $\tilde{\Omega}(\tau)$ has been used. There does not seem to be much effect on the numerical result when doing this in general, however, there is a visible difference at the end, where it is apparent that $|c_3|^2$ with the subtraction lies significantly closer to $|c_-|^2$. This makes sense, as the subtractions ensures that $\tilde{\Omega}'(T) = 0$ which (in theory) results in exactly $c_- = c_3$ at the end of the pulse. Some regular dips appear for $|c_-|^2$, which are not present in the garphs for $|c_3|^2$. This is in contrast with the dip found at $\sigma \sim 0.025$ which appears in all the different descriptions. Last, it seems like the bare state coefficient, both with and without subtraction, exhibits a higher degree of numerical error, i.e. the irregular jumps up and down, than the dressed state coeffcient. This might be the reason why the regular dips is not present in the bare state description.

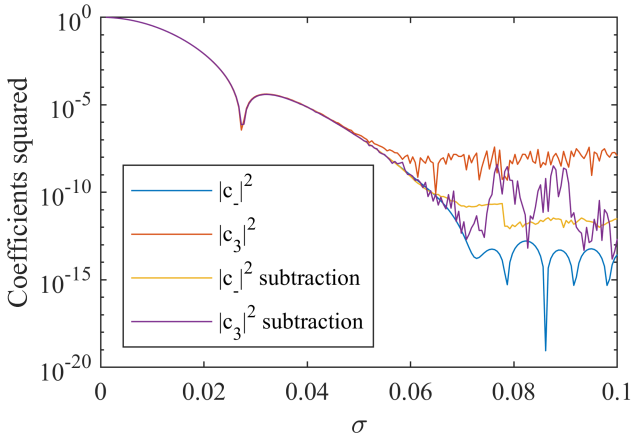


Figure 7: The numerical solutions of $|c_-|^2$ and $|c_3|^2$ together with the numerical solutions for differential euations where $\tilde{\Omega}'(\tau) = \tilde{\Omega}(\tau) - \tilde{\Omega}(T)$ has been used. They are depicted as functions of $\sigma$ for $\beta = 10$ and $\tilde{\Delta} = 100$.

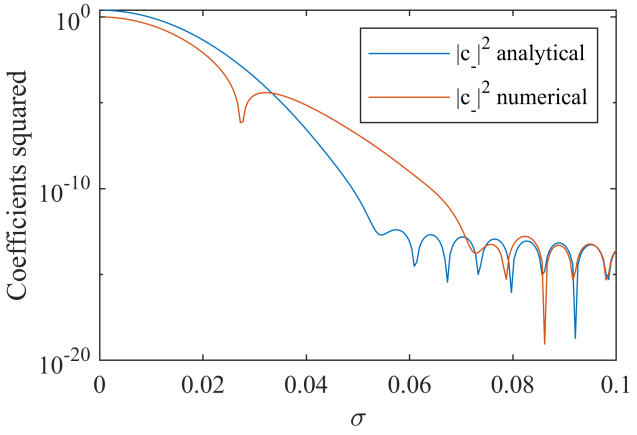


Figure 8: Comparison of the numerical and analytical solutions of the differential equations written in the basis of the dressed states. Here as functions of $\sigma$ and wiht $\beta = 10$ and $\tilde{\Delta} = 100$.

## 5.2 Solution for the dressed state coefficient

The equations 92 and 93 cannot be solved analytically, and therefore some approximations must be made. The first is in reference to figure 6. As $|c_+|^2$ is almost constant, it should be reasonable to set $c_+ = 1$ in the differential equation describing $c_-$. In this way the expression for $c_-$ can be found by solving an integral rather than a differential equation.

$$c_-(\tau) = -\frac{\alpha}{2\sqrt{2\pi}\sigma^3} \int_0^\tau \frac{\tilde{\Delta}}{\tilde{\Omega}^2 + \tilde{\Delta}^2} (\tau - \mu)\, \mathrm{e}^{-i\int_0^{\tau'}\sqrt{\tilde{\Omega}^2+\tilde{\Delta}^2}d\tau''}\, \mathrm{e}^{-\left(\frac{\tau-\mu}{\sqrt{2}\sigma}\right)^2} d\tau \tag{99}$$

This integral is too complicated to be solved analytically and thus more approximations are needed. It is therefore supposed that $\tilde{\Delta} >> \tilde{\Omega}$. As the pulse needed for the protocol is a $\pi$-pulse, the integral of $\tilde{\Omega}$ during the pulse is equal to $\pi$, and this approximation of a small $\tilde{\Omega}$ corresponds to supposing relatively long pulse durations, $T$. This approximation enables the following simplifications.

$$\frac{\tilde{\Delta}}{\tilde{\Omega}^2 + \tilde{\Delta}^2} \approx \frac{1}{\tilde{\Delta}} \quad \text{and} \quad \int_0^{\tau'} \sqrt{\tilde{\Omega}^2 + \tilde{\Delta}^2} d\tau'' \approx \tilde{\Delta} \int_0^{\tau'} d\tau'' = \tilde{\Delta}\, \tau' \tag{100}$$

These are inserted into equation 99.

$$c_-(\tau) = -\frac{\alpha}{2\sqrt{2\pi}\sigma^3} \frac{1}{\tilde{\Delta}} \int_0^\tau (\tau' - \mu)\, \mathrm{e}^{-i\Delta\tau'}\, \mathrm{e}^{-\left(\frac{\tau'-\mu}{\sqrt{2}\sigma}\right)^2} d\tau' \tag{101}$$

$$= -\frac{\alpha\, \mathrm{e}^{-i\tilde{\Delta}\mu}}{2\sqrt{2\pi}\sigma^3\tilde{\Delta}} \int_0^\tau (\tau' - \mu)\, \mathrm{e}^{-i\tilde{\Delta}(\tau'-\mu)}\, \mathrm{e}^{-\left(\frac{\tau'-\mu}{\sqrt{2}\sigma}\right)^2} d\tau' \tag{102}$$

A change of variables is made by using $\chi = \frac{\tau}{\sigma} \Rightarrow \frac{d\chi}{d\tau} = \frac{1}{\sigma}$ and $\frac{\mu}{\sigma} = \frac{\beta}{2}$ is used.

$$c_-(\chi) = -\frac{\alpha\, \mathrm{e}^{-i\tilde{\Delta}\mu}}{2\sqrt{2\pi}\sigma^3\tilde{\Delta}} \int_0^\chi (\sigma\chi' - \mu)\, \mathrm{e}^{-i\tilde{\Delta}(\sigma\chi'-\mu)}\, \mathrm{e}^{-\left(\frac{\sigma\chi'-\mu}{\sqrt{2}\sigma}\right)^2} \sigma\, d\chi' \tag{103}$$

$$= -\frac{\alpha\, \mathrm{e}^{-i\tilde{\Delta}\mu}}{2\sqrt{2\pi}\sigma\tilde{\Delta}} \int_0^\chi \left(\chi' - \frac{\beta}{2}\right) \mathrm{e}^{-i\tilde{\Delta}\sigma\left(\chi'-\frac{\beta}{2}\right)}\, \mathrm{e}^{-\left(\frac{\chi'-\frac{\beta}{2}}{\sqrt{2}}\right)^2} d\chi' \tag{104}$$

The identity $\mathrm{e}^{ix} = \cos(x) + i\, \sin(x)$ is used.

$$c_-(\chi) = -\frac{\alpha\, \mathrm{e}^{-i\tilde{\Delta}\mu}}{2\sqrt{2\pi}\sigma\tilde{\Delta}} \int_0^\chi \left(\chi' - \frac{\beta}{2}\right) \left(\cos\left(\tilde{\Delta}\sigma\left(\chi' - \frac{\beta}{2}\right)\right) + i\, \sin\left(\tilde{\Delta}\sigma\left(\chi' - \frac{\beta}{2}\right)\right)\right) \mathrm{e}^{-\left(\frac{\chi'-\frac{\beta}{2}}{\sqrt{2}}\right)^2} d\chi' \tag{105}$$

The cosine term is symmetric around $\chi - \frac{\beta}{2}$. When multiplied with the anti-symmetric $\chi - \frac{\beta}{2}$ and the symmetric exponential term, the result is something which is anti-symmetric around $\chi - \frac{\beta}{2}$. The integral of this is zero. The sine, however, is anti-symmetric, and as the product of two anti-symmetric functions is a symmetric one, the integral will be of a symmetric function, and will therefore not be zero. These considerations only apply when the integral is taken over equal intervals on either side of $\chi - \frac{\beta}{2}$, as is the case when the integral is taken over the entire length of the pulse. This restriction is not a problem as it is not necessary to know how $c_-$ changes during the pulse, but only its value at the end, where $|-\rangle = |3\rangle$. The end of the pulse, $\tau = T$, corresponds to $\chi = \frac{T}{\sigma} = \beta$. By implementing these considerations, the expression is reduced in the following way.

$$c_-(\chi) = -\frac{i\,\alpha\, \mathrm{e}^{-i\tilde{\Delta}\mu}}{2\sqrt{2\pi}\sigma\tilde{\Delta}} \int_0^\beta \left(\chi' - \frac{\beta}{2}\right) \sin\left(\tilde{\Delta}\sigma\left(\chi' - \frac{\beta}{2}\right)\right) \mathrm{e}^{-\left(\frac{\chi'-\frac{\beta}{2}}{\sqrt{2}}\right)^2} d\chi' \tag{106}$$

Another change of variables $\xi = \chi - \frac{\beta}{2}$ is made. By this, the upper limit of the integral becomes $\beta - \frac{\beta}{2} = \frac{\beta}{2}$.

$$c_-(\xi) = -\frac{i\,\alpha\, \mathrm{e}^{-i\tilde{\Delta}\mu}}{2\sqrt{2\pi}\sigma\tilde{\Delta}} \int_{-\frac{\beta}{2}}^{\frac{\beta}{2}} \xi\, \sin\left(\tilde{\Delta}\sigma\xi\right) \mathrm{e}^{-\frac{\xi^2}{2}}\, d\xi' \tag{107}$$

This expression is simple enough to be solved analytically by calculation software, and the result is shown in equation 108. Here $\mu = \frac{\sigma\beta}{2}$ has been used.

$$c_- = -\frac{\alpha}{4\sqrt{2\pi}\sigma\tilde{\Delta}} e^{-i\frac{1}{2}\sigma\tilde{\Delta}\beta} e^{-\frac{1}{2}\sigma^2\tilde{\Delta}^2} \left( 2e^{\frac{1}{8}(2\sigma\tilde{\Delta}-i\beta)^2} - 2e^{\frac{1}{8}(2\sigma\tilde{\Delta}+i\beta)^2} - \sqrt{2\pi}\sigma\tilde{\Delta}\,\mathrm{erfi}\left(\frac{2\sigma\tilde{\Delta}-i\beta}{2\sqrt{2}}\right) + \sqrt{2\pi}\sigma\tilde{\Delta}\,\mathrm{erfi}\left(\frac{2\sigma\tilde{\Delta}+i\beta}{2\sqrt{2}}\right)\right) \tag{108}$$

In figure 8 this expression is plotted together with the numerical solution to the differential equations for the dressed states. It can be concluded that this analytical description of the coefficients do not make a good description either, as it do not fit the numerical solution. Only for very high values of $\sigma$ does the numerical and analytical solutions correspond.

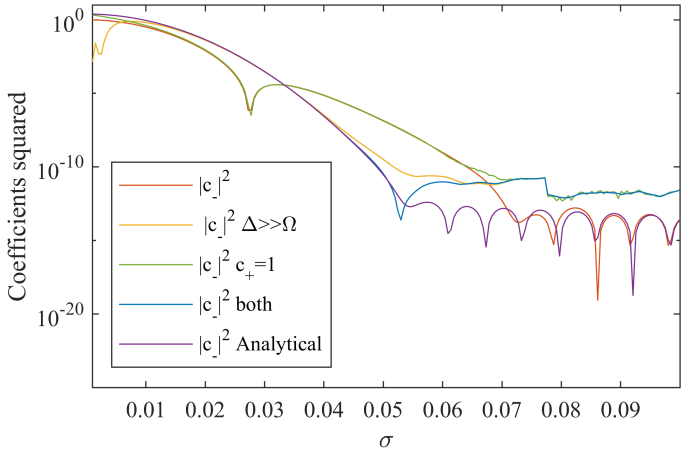


Figure 9: Together with the numerical and analytical solution in the dressed state basis is the numerical solutions of differential equations where the different approximations has been implemented. The graphs are shown as functions of $\sigma$ and with $\beta = 10$ and $\tilde{\Delta} = 100$.

The problem of the analytical solution not fitting the numerical must lie with one or both of the approximations as the shift to the dressed state picture itself has been shown to be fine. To investigate this figure 9 compares numerical solutions of the differential equations, where the different approximations has been applied.

As can be seen in figure 9, using $c_+ = 1$ in the equation for $c_-$ still results in values of $|c_-|^2$ that are very close to the full solution of the differential equations. It is therefore justifiable to rewrite the differential equation as an integral, thereby making a significant step towards finding an analytical description of the system. The other approximation, $\tilde{\Delta} >> \tilde{\Omega}$, however, does not seem to work very well. The results of implementing this in the differential equations are similar to the analytical result, and do not resemble the numerical solution. The exception is values of $\sigma > 0.08$, where the numerical and analytical solutions corresponds almost exactly. By this it can be concluded that the approximation $\tilde{\Delta} >> \tilde{\Omega}$ does only hold for pulses that are broader than this value. At $\sigma = 0.08$ the maximum of $\tilde{\Omega}$ is $\tilde{\Omega}(\mu) = \frac{\alpha}{\sqrt{2\pi}\sigma} = 15.7$ and is thus about a sixth of $\tilde{\Delta} = 100$, which is the value used in these plots. As is apparent in figure 10, where the numerical solution for different values of $\beta$ is plotted, the only significant effect of $\beta$ is to determine at what value this flattened out area begins.

Thus it can be concluded that the dressed state analytical solution in 108 does not describe the system well, except in the regime which is dominated by $\beta$ error.

## 5.3 Further investigations

As it has not been possible to find an analytical expression describing the system, a fit is made to the numerically found values of $c_3(T)$ for different values of $\sigma$. A Gaussian function as given in equation 109 is fitted to the numerical

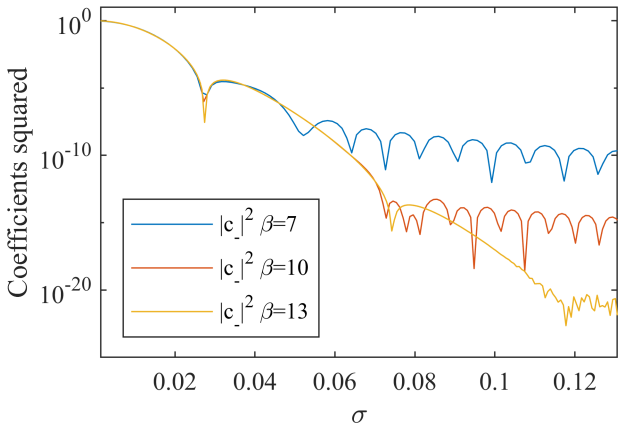


Figure 10: The numerical solution of the dressed state coefficient as a function of $\sigma$ for different values of $\beta$ and with $\tilde{\Delta} = 100$.

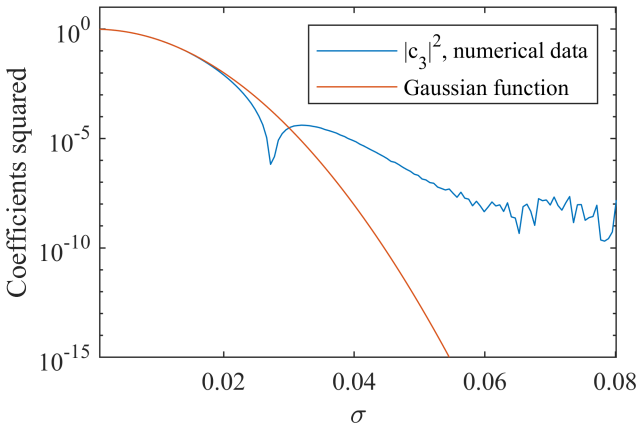


Figure 11: A Gaussian function has been fitted to the numerical solution of the bare state coefficients with respect to $\sigma$. Here with $\beta = 10$ and $\tilde{\Delta} = 100$.

values in figure 11.

$$|c(\sigma)|^2 = A\, \mathrm{e}^{-\frac{(\sigma - B)^2}{C}} \tag{109}$$

The fit works very well for small values of $\sigma$, which means that $|c_3|^2$ goes as a Gaussian function in this regime. The parameters of the fit are given in equation 110.

$$\begin{aligned} A &= 0.9943 \pm 9\,10^{-4} \\ B &= 1.9\,10^{-4} \pm 0.2\,10^{-4} \\ C &= 8.58\,10^{-5} \pm 0.02\,10^{-5} \end{aligned} \tag{110}$$

As $B$ only serves to move the mean values of the Gaussian function away from zero (and is very small), the fit can be said to be proportional to $\mathrm{e}^{-\frac{\sigma^2}{C}}$. This can be compared to the analytical expression for $c_3$ given in equation 71, where $|c_3|^2 \propto \mathrm{e}^{\sigma^2 \tilde{\Delta}^2}$. Thus the factor of $\frac{1}{C} = 1.17\,10^4$ in the exponent can be compared to $\tilde{\Delta}^2 = 1\,10^4$ in the analytical solution of $c_3$. In order to make this comparison with the analytical expression of $c_-$ as well, it must be rewritten on the form of $\propto \mathrm{e}^{-a\,\sigma^2}$. This is not simple to do, however, if one takes the limit for $\beta \to$ the expression in 108 becomes the following.

$$c_- \approx i\frac{\alpha}{2}\mathrm{e}^{-i\frac{1}{2}\tilde{\Delta}\sigma\beta}\ \mathrm{e}^{-\frac{1}{2}\sigma^2\tilde{\Delta}^2} \Rightarrow |c_-|^2 \approx \frac{\alpha^2}{4}\mathrm{e}^{-\sigma^2\tilde{\Delta}^2} \tag{111}$$

This is the same expression as the one found for the bare state description, as $\alpha \approx \pi$, meaning that as $\beta \to$ the two analytical descriptions become the same. This corresponds with figure 10 which shows that as $\beta \to$ the flattened area moves down. The two analytical expressions follow each other closely up until the point where this behaviour begins as is shown in figure 12. This indicates that they should indeed become the same for all $\sigma$.

There are sources of error from both $\sigma$, that arises from the nature of the pulse and therefore the physical system, and $\beta$, that arises from the cutting off of the pulse. To investigate this a contour plot is made with the analytical endvalues $|c_3|^2$ for different values of $\sigma$ and $\beta$. This is explored in figure 13, where a surface plot shows that for the larger values of $\beta$ the same profile is seen as in the plots for a specific $\beta$; as $\sigma$ becomes larger, $|c_3|^2$ drops from one towards zero. The characteristic dip at $\sigma \sim 0.025$ appears at the same place for different values of $\beta$. This implies that it is not an effect caused by the cutting off of the pulse, but is an effect of the physical system, a $\sigma$ error. Complex behaviour like this might be one of the reasons why it is so difficult to obtain a simple, analytical description of the system. The point at which $|c_3|^2$ flattens out and stops going towards zero, $\sigma \sim 0.05$, also seems to be the same for most values of $\beta$. For small values of $\beta$, however, the picture completely changes and oscillations appear. This is caused by the fact that very small values of $\beta$, in combination with not too small values

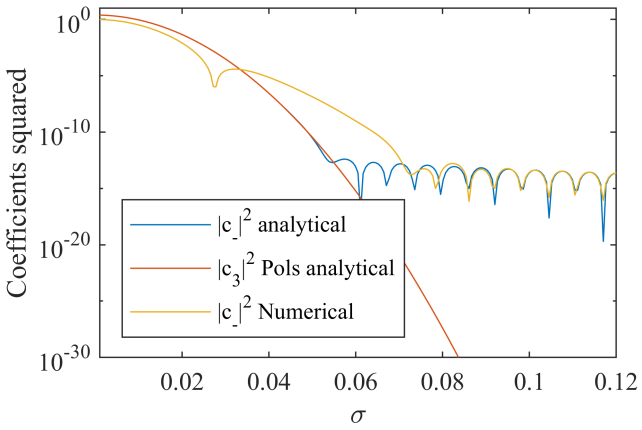


Figure 12: The analytical solutions in the bare and dressed state basis respectively plotted together with the numerical solution (in the dressed state basis). Here with $\beta = 10$ and $\tilde{\Delta} = 100$.

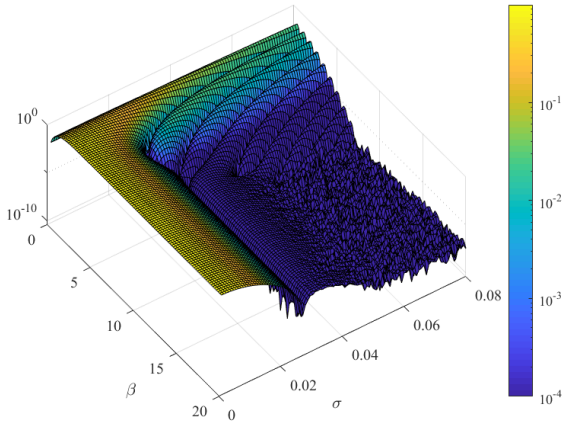


Figure 13: A surface plot showing the numerical solution of $|c_3|^2$ as a function of $\sigma$ and $\beta$ with $\tilde{\Delta} = 100$.

of $\sigma$, means that the pulse will be cut off close to its maximum, and thus resembles a square pulse. A square pulse will result in Rabi oscillations [10]. The limit between the Gaussian description of the system and the regime where it exhibits oscillations, appears at around $\beta \sim 5$.

## 5.4 Spontaneous decay

Something, which has not been taken into consideration in the previous parts, but which will have an impact on the state of the system, is spontaneous decay from $|3\rangle$ to some other level than $|0\rangle$. Such a decay would modify the equations of motion (equation 34) with a term, $-\frac{1}{2}c_3$ corresponding to that in the differential equation for the excited state in the resonant transition (equation 36), where spontaneous decay is already taken into account, as it forms a part of the protocol. The new differential equations are presented in equation 112 and 113.

$$\dot{c_3}(\tau) = i\frac{\tilde{\Omega}_3(\tau)_3}{2}c_0(\tau) - i\tilde{\Delta}c_3(\tau) - \frac{1}{2}c_3(\tau) \tag{112}$$

$$\dot{c_0}(\tau) = i\frac{\tilde{\Omega}_3(\tau)_3^*}{2}c_3(\tau) \tag{113}$$

The differential equations will not be solved here, and the effect of the decay term will merely be approximated. With the possibility of spontaneous decay, one no longer has $|c_0|^2+|c_3|^2= 1$, but instead the following.

$$|c_0|^2+|c_3|^2+P(decay) = 1 \tag{114}$$

Here $P(decay)$ is the probability of spontaneous decay of $|3\rangle$ to some other state. The ideal system would have $|c_0|^2= 1$ as this means that there is no probability of driving the far-detuned transition. When previously calculating $|c_3|^2$ it has been in order to calculate the error to this assumption, that is calculating $1 - |c_0|^2$, which in the case of no spontaneous decay term is equal to $|c_3|^2$. Now however, the decay term is taken into account, and the error as given by equation 115 needs to be calculated.

$$1 - |c_0|^2= |c_3|^2+P(decay) \tag{115}$$

To calculate this some considerations must be made. For broard pulses, i.e. high values of $\sigma$, $|c_-|^2$ is very small, and it can be assumed that the system is always in the state $|+\rangle = \cos\frac{\theta}{2}\,|0\rangle + \sin\frac{\theta}{2}\,|3\rangle$. If the system is in this

dressed state, the probability of being in the bare state $|3\rangle$ is given by the coefficient $\sin\frac{\theta}{2}$ squared.

$$|c_3|^2 = \sin^2\frac{\theta}{2} = \sin^2\left(\arctan\frac{\theta}{2}\right) \approx \frac{1}{4}\frac{\tilde{\Omega}^2}{\tilde{\Delta}^2} \tag{116}$$

For this approximation, a second order Taylor expansion was made at $\frac{\tilde{\Omega}}{\tilde{\Delta}} = 0$, since $\tilde{\Omega}$ is small for large values of $T$. In order to calculate the probability of spontaneous decay, the integral of the decay term is taken.

$$P(decay) = 2\int_0^\tau \frac{1}{2}|c_3|^2\, d\tau' = \frac{1}{4\,\tilde{\Delta}^2}\int_0^t \tilde{\Omega}^2\, d\tau' = \frac{\alpha^2}{8\pi\sigma^2\tilde{\Delta}^2}\int_0^\tau \mathrm{e}^{-2\left(\frac{\tau'-\mu}{\sqrt{2}\sigma}\right)^2} d\tau' \tag{117}$$

A change of variables $\chi = \frac{\tau}{\sigma} \Rightarrow \frac{d\chi}{d\tau} = \frac{1}{\sigma}$ is made.

$$P(decay) = \frac{\alpha^2}{8\pi\sigma^2\tilde{\Delta}^2}\int_0^\chi \mathrm{e}^{-2\left(\frac{\chi'-\frac{\mu}{\sigma}}{\sqrt{2}}\right)^2}\sigma\, d\chi' = \frac{\alpha^2}{8\pi\sigma\tilde{\Delta}^2}\int_0^\chi \mathrm{e}^{-\left(\chi'-\frac{\beta}{2}\right)^2} d\chi' \tag{118}$$

And another change of variables $\xi = \chi - \frac{\beta}{2}$.

$$P(decay) = \frac{\alpha^2}{8\pi\sigma\tilde{\Delta}^2}\int_{-\frac{\beta}{2}}^{\chi-\frac{\beta}{2}} \mathrm{e}^{-\xi'^2}\, d\xi' \tag{119}$$

Instead of solving the integral with limits $-\frac{\beta}{2}$ to $\chi - \frac{\beta}{2}$, one can solve it with $\chi = \frac{T}{\sigma}$, which gives an upper limit of $\frac{\beta}{2}$. This is done as one is only interested in the values at the end of the pulse.

$$P(decay) = \frac{\alpha^2}{8\pi\sigma\tilde{\Delta}^2}\int_{-\frac{\beta}{2}}^{\frac{\beta}{2}} \mathrm{e}^{-\xi^2}\, d\xi = \frac{\alpha^2}{8\pi\sigma\tilde{\Delta}^2}\sqrt{\pi}\left(\mathrm{erf}\left(\frac{\beta}{2}\right)\right) \tag{120}$$

The final solution for $1 - |c_0|^2$ thus becomes as follows.

$$1 - |c_0(T)|^2 = \frac{\Omega^2}{4\Delta^2} + \frac{\alpha^2}{8\pi\sigma\tilde{\Delta}^2}\sqrt{\pi}\left(\mathrm{erf}\left(\frac{\beta}{2}\right)\right) \tag{121}$$

In figure 14 the approximated solution to $1 - |c_0|^2$ from equation 115 is plotted together with the numerical solution to the differential equations in 112 and 113 and the numerical solution to the differential equation to the differential equations without the decay term (equations 34 and 35). By first comparing the two numerical solutions, it is clear that having the possibility of spontaneous decay rises the value of $1 - |c_0|^2$ considerably. Some of the finer details of $c_3$, that occurs on the order of $\sim 10^{-5}$ might therefore be irrelevant, as these will drown in the effect of the decay term, which is roughly 100 times larger. Given that this is the case it seems that it is not a problem that the Gaussian function, which was fitted to the numerical data, only works very well at small values of $\sigma$, since details that appears for values of $\sigma > 0.025 - 0.03$ will be overruled by the error caused by spontaneous decay.

By secondly comparing the numerical result with the decay term and the approximated result, the approximations seem to hold for values of $\sigma$ that are higher than 0.03. It makes sense that the approximation breaks down for small values of $\sigma$, since the assumption that $\tilde{\Omega}$ is small no longer holds when the pulse is very narrow. The graphs of $P(decay)$ and $\frac{\tilde{\Omega}^2}{4\tilde{\Delta}^2} + P(decay)$ lie almost exactly on top of each other, meaning that up to the second order contribution to $|c_3|^2$ is almost zero, even for small values of $\sigma$. Thus, when taking spontaneous decay into consideration, there is practically no probability of the system being in state $|3\rangle$; if the system is excited by the far-detuned transition, it almost instantly decays to some other level.

## 5.5 Approximating in the opposite regime

The Gaussian function fits the numerical solution of $|c_3|^2$ well for small values of $\sigma$, and thus it might be advantageous to look at the system in this regime, which corresponds to $\tilde{\Delta} << \tilde{\Omega}$, and afterwards generalise to all values of $\sigma$. By this method it might be possible to get an expression for the coefficients.[11]

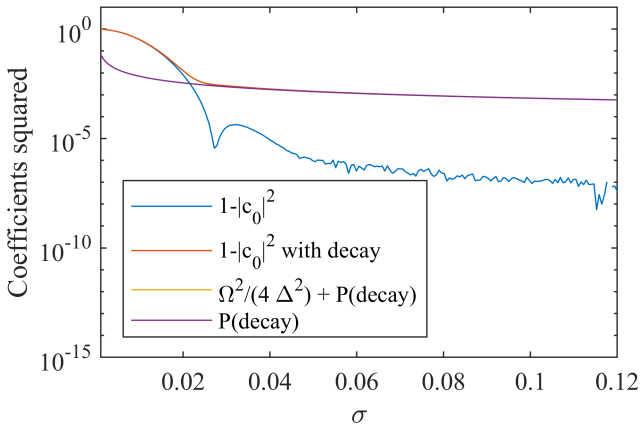


Figure 14: The numerical and approximate descriptions of the error, $1-|c_0|^2$, when spontaneous decay has been taken into consideration compared with the numerical solution with no spontaneous decay. Here as functions of $\sigma$ with $\beta = 10$ and $\tilde{\Delta} = 100$.

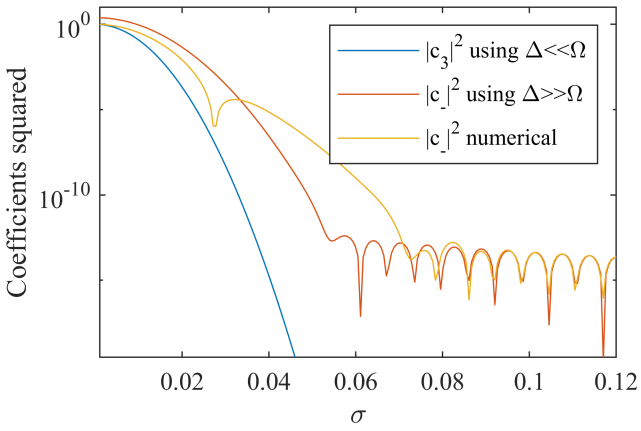


Figure 15: The numerical solutions of $|c_3|^2$ and $|c_-|^2$ and the analytical solution of $|c_-|^2$ compared with the description of $c_3$ found by using the approximation $\tilde{\Delta} << \tilde{\Omega}$. Here as functions of $\sigma$ and with $\beta = 10$ and $\tilde{\Delta} = 100$.

When $\sigma$ is very small, the Gaussian function takes the following form.

$$\mathrm{e}^{-\frac{\sigma^2}{C}} \approx 1 - \frac{\sigma^2}{C} \tag{122}$$

This means that if one can get $c_3$ on the form $1 - a\tilde{\Delta}^2\tilde{\sigma}^2$, where $a$ is some constant, when $\tilde{\Delta} << \tilde{\Omega}$, it is possible to generalise this expression to all values of $\sigma$ in the expression $|c_3|^2 = \mathrm{e}^{-a\tilde{\Delta}^2\sigma^2}$. In order to do this, perturbation around $\tilde{\Delta}$ is be made, as the functions are expanded in the following way.

$$c_3 = c_3^{(0)} + \tilde{\Delta}c_3^{(1)} + ... \tag{123}$$

$$c_0 = c_0^{(0)} + \tilde{\Delta}c_0^{(1)} + ... \tag{124}$$

By inserting this in the differential equations and collecting the terms, which has the same order of $\tilde{\Delta}$ one get the following differential equations for each order.

$$\dot{c}_3^{(N)} = -ic_3^{(N-1)} + i\frac{\tilde{\Omega}}{2}c_0^{(N)} \tag{125}$$

$$\dot{c}_0^{(N)} = i\frac{\tilde{\Omega}}{2}c_3^{(N)} \tag{126}$$

These are the same equations as those solved in [10] for the resonant transition except for the factor of $i$ on the term with $c_3^{(N-1)}$. The zeroth order equations are therefore exactly the same and the solutions are presented in equations 127 and 128 with reference to [10] for the method.

$$c_3^{(0)} = i\sin\left(\frac{1}{2}\int_0^\tau \tilde{\Omega}d\tau\right) \tag{127}$$

$$c_0^{(0)} = \cos\left(\frac{1}{2}\int_0^\tau \tilde{\Omega}d\tau\right) \tag{128}$$

Despite the factor of $i$, the solutions of the first order equations are also parallel to what is done for the resonant transition in [10]. With reference to this work therefor, the following integral describing the coefficient of the excited

level is presented. The zeroth order expression of $c_3$ is inserted.

$$c_0^{(1)} = -i \int_0^T \sin\left(\frac{1}{2}\int_0^\tau \tilde{\Omega} d\tau\right) c_3^{(0)} d\tau = \int_0^T \sin^2\left(\frac{1}{2}\int_0^\tau \tilde{\Omega} d\tau\right) d\tau \tag{129}$$

A change of variables is made with $\xi = \frac{\tau-\mu}{\sigma} \Rightarrow \frac{d\xi}{dt} = \frac{1}{\sigma}$. This gives a lower limit on the integral of $\xi(0) = \frac{\mu}{\sigma} = \frac{\beta}{2}$ and an upper limit (in the case of $\tau = T$) of $\xi(T) = \frac{T-\mu}{\sigma} = \frac{\beta}{2}$.

$$c_0^{(1)} = \sigma \int_{-\frac{\beta}{2}}^{\frac{\beta}{2}} \sin^2\left(\frac{\alpha}{\sqrt{2\pi}} \int_{-\frac{\beta}{2}}^{\xi} \mathrm{e}^{-\xi^2/2} d\xi\right) d\xi \tag{130}$$

$$= \sigma \int_{-\frac{\beta}{2}}^{\frac{\beta}{2}} \sin^2\left(\frac{\alpha}{2}\left(\mathrm{erf}\left(\frac{\beta}{2\sqrt{2}}\right) + \left(\mathrm{erf}\left(\frac{\xi}{\sqrt{2}}\right)\right)\right)\right) d\xi = \sigma \cdot \mathrm{INT} \tag{131}$$

This integral, here called INT, cannot be solved analytically, however it can be done numerically. As both the zeroth and first order terms have now been found, the expression for $c_0$ can be written down. Below, the fact that the integral over $\tilde{\Omega}$ from 0 to $T$ is equal to $\pi$ has been used.

$$c_0 \approx c_0^{(0)} + \tilde{\Delta} c_0^{(1)} = \cos\left(\frac{1}{2}\int_0^T \tilde{\Omega} d\tau\right) + \tilde{\Delta}\sigma\,\mathrm{INT} = \cos\frac{\pi}{2} + \tilde{\Delta}\sigma\,\mathrm{INT} = \tilde{\Delta}\sigma\,\mathrm{INT} \tag{132}$$

$$\Rightarrow |c_0|^2 = \tilde{\Delta}^2\sigma^2\,\mathrm{INT}^2 \tag{133}$$

As no spontaneous decay is taken into account $|c_0|^2 + |c_3|^2 = 1$ and thus $|c_3|^2$ can be found and generalised.

$$|c_3|^2 = 1 - |c_0|^2 = 1 - \tilde{\Delta}^2\sigma^2\,\mathrm{INT}^2 \Rightarrow |c_3|^2 = \mathrm{e}^{\tilde{\Delta}^2\sigma^2\,\mathrm{INT}^2} \tag{134}$$

In figure 15 the expression in 134 is plotted together with the numerical solution and the analytical (dressed state) solution, i.e. equation 108. It is clear that the expression found here only lies close to the numerical solution for very small values of $\sigma$ and does not in general make for a good description of the system.

# 6 Conclusion

Moving to a dressed state basis for the description of the far-detuned transition makes physical sense and has the advantage of enabling the rewriting of the differential equations describing the coefficients as an integral. Unfortunately this integral cannot be solved analytically without approximations that do not in general hold. Investigation of the numerical solutions reveals complex behaviour and no good method of describing the system has been found. The possibility of spontaneous decay from the upper level of the far-detuned system has been found to change the system significantly.

# References


[1] *Cryo-CMOS Electronic Control for Scalable Quantum Computing: Invited - Scientific Figure on ResearchGate*, 01 2020. URL `https://www.researchgate.net/figure/Bloch-sphere-representation-of-a-qubit_fig1_317573486`.

[2] Stephen M. Barnett. *Quantum Information*. Oxford Master Series in Atomic, Optical and Laser Physics. Oxford University Press, 2009.

[3] K. F. Riley & M. P. Hobson. *Essential Mathematical Methods for the Physical Sciences*.

[4] Christopher J. Foot. *Atomic Physics*. Oxford Master Series in Atomic, Optical and Laser Physics. Oxford University Press, 2005.

[5] Tim Schröder Mikhail D. Lukin Peter Lodahl & Anders S. Srensen Johannes Borregaard, Hannes Pichler. One-way quantum repeater based on near-deterministic photon-emitter interfaces. 07 2019.

[6] Jungsang Kim Norbert Lutkenhaus Mikhail D. Lukin & Liang Jiang Sreraman Muralidharan1, Linshu Li. Effcient long distance quantum communication. 09 2015.

[7] Daniel E. Browne & Terry Rudolph Michael Varnava. Loss tolerance in one-way quantum computation via counterfactual error correction. *Physical Review Letters*, 97(120501), 09 2006.

[8] A. J. Bennett R. M. Stevenson D. J. P. Ellis I. Farrer D. A. Ritchie & A. J. Shields J. P. Lee, B. Villa. Towards a source of multi-photon entangled states for linear optical quantum computing. 05 2018.

[9] Terry Rudolph. Why i am optimistic about the siliconphotonic route to quantum computing. *APL Photonics 2*, (030901), 06 2017.

[10] Pol Llopart Mirambell. *Fidelity characterization of spin-photon entangled states*, 07 2019.

[11] David J. Griffiths. *Introduction to Quantum Mechanics*. Second edition.

[12] *Lecture Notes for Quantum Optics 2*, 04 2013.